Pergamon

0301-9322(95)00058-5

Int. J. Multiphase Flow Vol. 22, No. 1, pp. 93–120, 1996

0301-9322/96 $15.00 + 0.00

NUMERICAL SIMULATION OF THE DYNAMICS OF AN ELECTROSTATICALLY LEVITATED DROP†

Z. C. FENG[1] and L. G. LEAL[2]

[1]Department of Mechanical Engineering, Massachusetts Institute of Technology, Cambridge, MA 02139, U.S.A.

[2]Department of Chemical and Nuclear Engineering, University of California, Santa Barbara, CA 93106, U.S.A.

(Received 13 January 1995; in revised form 22 June 1995)

Abstract—In this paper we use the boundary integral method to simulate the dynamics of a liquid drop levitated by electrostatic force. Our numerical code reproduces the Rayleigh limit, the Taylor limit and the stable equilibrium shape of a leviated drop obtained by previous authors. It also reveals the mechanism by which a levitated drop might breakup. Using this code, we have obtained the natural frequencies of the drop under various levitation conditions. We have also examined the effect of the electrostatic field on the resonant interactions between the modes. We found that the presence of the electric field enhances the modal interactions; modes which otherwise would not interact become coupled to each other. Calculations of the dynamics of a levitated drop under a time-periodic electric field indicate that the main resonance occurs when the frequency of the electric field is near the free oscillation frequency of the fundamental mode.

Key Words: drop dynamics, electrostatic levitation, shape oscillation, boundary element method

1. INTRODUCTION

With the development of techniques for levitating a large drop by electrostatic forces (Rhim *et al.* 1987), new experiments on drop dynamics and related applications in various fields have become possible. In the meantime, a significant amount of theoretical work on the dynamics of charged drops in an electric field has also been done in the last decade. One topic has been numerical computation of the drop equilibrium shape, including work done by Miksis (1981), Adornato & Brown (1983), Basaran & Scriven (1989a, b) and Pelekasis & Tsamopoulos (1990). Another set of studies has been concerned with the dependence of drop dynamics on the electric charge on the drop, or on the magnitude of the applied electric field. These latter studies have used primarily asymptotic expansions coupled with domain perturbations from a spherical base case. Specific examples include the work of Feng & Beard (1990, 1991a, b) and Kang (1993), who studied the dependence of drop oscillation frequencies on the magnitude of the electric charge or the applied electric field. Tsamopoulos & Brown (1984) studied resonant coupling between the normal modes, while Tsamopoulos *et al.* (1985) and Natarajan & Brown (1987) studied drop breakup due to the electric charge or electric field. Due to the perturbative nature of the approach, these analyses and results are typically applicable only in some small domain of parameter space.

Interestingly, an analytical approach based on a spheroidal base case has been very successful in predicting the drop equilibrium shape (Basaran & Scriven 1989) and natural frequencies of the fundamental mode (Brazier-Smith *et al.* 1971) for cases where the actual shape is not a near sphere. The spheroidal approximation method (Taylor 1964) assumes that the shape of the drop is spheroidal and applies boundary conditions only at the poles and the equator in order to determine the aspect ratio. Recently, Kang (1993) has used the spheroidal approximation to study drop breakup in an axisymmetric, time periodic electric field with fore–aft symmetry.

The spheroidal approximation yields concise yet quite accurate results for the equilibrium shape and resonance frequencies for drops with spheroidal symmetry. However, it cannot be applied to study the dynamics of a levitated drop because the latter does not have *mirror* symmetry about

†This research was supported by NASA.

the equator and its shape cannot be approximated by a spheroid. Thus, apart from the asymptotic results of Feng & Beard (1990), fundamental questions about the dynamics of a levitated drop, such as the resonance frequencies and energy transfer mechanism between modes, remain to be answered.

In this paper, we use numerical simulations to study the dynamics of an electrostatically levitated conducting liquid drop under normal gravitational conditions. The numerical method we use is the boundary element method. We reproduce previous results with regard to the Rayleigh limit, the Taylor limit and the drop equilibrium shape. In addition, we show that the time evolution of the drop dynamics is strongly dependent upon the initial shape of the drop. Our calculation of the natural oscillation frequencies of a levitated drop extend existing perturbation results to cover all stable parameter values. We also conduct a preliminary study of the drop dynamics in the presence of a time-periodic electric field.

The dynamics of a liquid drop in an electric field is an interesting fundamental topic in the physics of fluids. Beyond this, an understanding of non-linear phenomena can have an important impact on implementation of material processing techniques in microgravity. Furthermore, the latest research activities have also been stimulated by possible application in electrospray ionization (Gomez & Tang 1994).

2. MATHEMATICAL FORMULATION

We consider an axisymmetric conducting drop of volume $(4\pi/3)R^3$, density ρ, uniform interfacial tension σ and net electrical charge Q^*, levitated in a tenuous insulating medium by an external uniform electrostatic field E_0^* applied in the opposite direction to the gravitational acceleration $\boldsymbol{g}$. The insulating medium has electric permittivity ϵ_m. We assume that the flow inside the drop is a potential flow with velocity potential ϕ^*. Let E^* and V^* denote the electric field and the electrostatic potential. In a cylindrical coordinate shown in figure 1, we choose R, $\sqrt{(\rho R^3/\sigma)}$ and

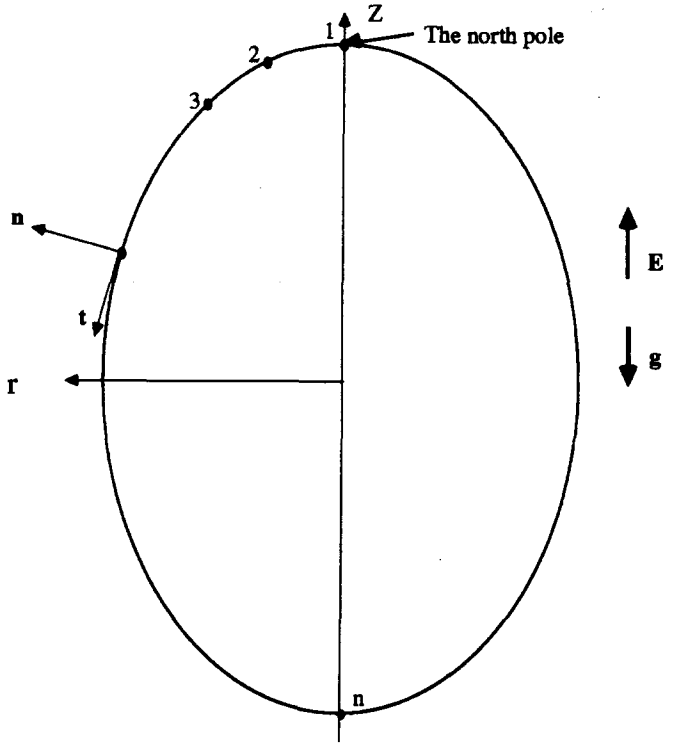

Figure 1. Coordinate axes.

Table 1. Non-dimensionalization used in various papers

Characteristic variables	Feng & Beard (1990)	Basaran & Scriven (1989)	Tsamopoulos & Brown (1984)	Lundgren & Mansour (1988)
t_c	$(\rho R^3/\sigma)^{1/2}$	—	$(\rho R^3/\sigma)^{1/2}$	$(\rho R^3/2\sigma)^{1/2}$
l_c	R	R	R	R
p_c	σ/R	σ/R	$2\sigma/R$	σ/R
E_c	$(\sigma/\epsilon_m R)^{1/2}$	$(2\sigma/\epsilon_m R)^{1/2}$	$(\sigma/4\pi\epsilon_m R)^{1/2}$	—
Q_c	$(\epsilon_m \sigma R^3)^{1/2}$	$(2\epsilon\sigma R^3)^{1/2}$	$(4\pi\epsilon_m \sigma R^3)^{1/2}$	—

σ/R as characteristic length, time and pressure. Following the same non-dimensionlization as in Feng & Beard (1990), we let:

$$\phi = \phi^* \sqrt{(\rho/\sigma R)},\ V = V^* \sqrt{(\epsilon_m/\sigma R)},$$
$$E = E^* \sqrt{(\epsilon_m R/\sigma)},\ Q = Q^*/\sqrt{(\epsilon_m \sigma R^3)}.$$

These non-dimensionalizations are compared with those of others in table 1.

The equation governing the hydrodynamic field for (z, r) within the drop is

$$\nabla^2 \phi = 0 \qquad [1]$$

The equation governing the electric field for (z, r) outside the drop is

$$\nabla^2 V = 0 \qquad [2]$$

On the drop surface, we have the normal stress balance:

$$\frac{\partial \phi}{\partial t} + \mathrm{B}z + \frac{1}{2}(\nabla\phi)^2 + \nabla\cdot\mathbf{n} - \frac{1}{2}(\nabla V)^2 = \Delta p_0 \qquad [3]$$

and since the drop is a conductor, the boundary condition for V is

$$V = V_0 \qquad [4]$$

where V_0 is a constant. The parameter B, which appears in [3] is the Bond number,

$$\mathrm{B} = \rho g R^2/\sigma \qquad [5]$$

which represents the magnitude of the gravity relative to the surface tension force. To gain some intuitive understanding, we note that for a water drop at 1 g, with $\rho = 1$ g/cm^3, $\sigma = 75$ dyne/cm and $g = 980$ cm/s^2, a Bond number $\mathrm{B} = 1$ corresponds to a diameter of 5.5 mm. The pressure adjustment Δp_0 may be time dependent, and is determined from the constraint of volume conservation of the drop. In addition, we have

$$V = -E_0 z \text{ at } r_0 \to \infty \qquad [6]$$

and the conservation of the total charge on the drop surface

$$-2\pi \int_0^\pi (\mathbf{n}\cdot\nabla V) r \, \mathrm{d}s = Q \qquad [7]$$

We do not write down the kinematic boundary condition for the time being. However, this boundary condition will be used to update the free surface in our numerical implementation to be discussed in the following.

3. BOUNDARY ELEMENT FORMULATION

We use the well-known boundary integral (boundary element) method in this work. Since the governing partial differential equations are simply Laplace equations for both the velocity potential and the electric potential, we can use the boundary integral formulation to establish the relationship between the two potentials, ϕ and V, and their normal derivatives on the boundary, ϕ_n and V_n. Our steps are the following. Given an initial shape of the free surface, we solve an electrostatic problem and a potential flow problem using the boundary element formulation. Once this is done, we use the normal stress boundary condition coupled with the kinematic boundary condition to

update the free surface shape and the velocity potential at the surface. This strategy amounts to numerical integration of the following dynamical systems at each time step:

$$\dot{z} = \phi_t t_z + \phi_n n_z \quad [8]$$

$$\dot{r} = \phi_t t_r + \phi_n n_r \quad [9]$$

$$\dot{\phi} = -\mathrm{B}z + \frac{1}{2}(\nabla\phi)^2 - \nabla\cdot\mathbf{n} + \frac{1}{2}(\nabla V)^2 \quad [10]$$

where $\mathbf{t} = t_z\mathbf{i}_z + t_r\mathbf{i}_r$ and $\mathbf{n} = n_z\mathbf{i}_z + n_r\mathbf{i}_r$ are the tangent and outward normal vectors respectively, $\mathbf{i}_z$ and $\mathbf{i}_r$ are the two unit vectors in the cylindrical coordinates, and $\nabla\cdot\mathbf{n}$ is the total curvature of the surface given by

$$\nabla\cdot\mathbf{n} = -\frac{z'(s)[z'(s)^2 + r'(s)^2] - r(s)[r''(s)z'(s) - r'(s)z''(s)]}{r(s)[z'(s)^2 + r'(s)]^{3/2}}$$

where s is the arclength measured from the node 1 in figure 1.

The boundary element formulation for axisymmetric problems is detailed in Brebbia *et al.* (1984). For the hydrodynamic problem, it establishes the relationship between the velocity potential and its normal derivatives on the boundary. If we discretize the axisymmetric free surface into $N-1$ elements and use linear interpolation to describe values of ϕ and ϕ_n in terms of the corresponding values at the N nodes, namely ϕ_1, ϕ_2, etc., the boundary element formulation gives us a linear system of equations:

$$\mathbf{G}\phi_n = \mathbf{H}\phi \quad [11]$$

where $\phi_n = ((\phi_n)_1, (\phi_n)_2, \ldots, (\phi_n)_N)^t$, $\phi = (\phi_1, \phi_2, \ldots, \phi_N)^t$ and matrices $\mathbf{G}$ and $\mathbf{H}$ depend only on the geometry of the free surface.

Once the matrices $\mathbf{G}$ and $\mathbf{H}$ have been formulated for the hydrodynamic problem, only slight modification of these matrices is needed in order to adapt them to solve the electrostatic problem, because if we write

$$V^\infty = -E_0 z$$

we can decompose V into

$$V = V^s + V^\infty$$

Obviously V^s satisfies the Laplace equation and

$$V^s = 0$$

at infinity.

Since the total electric potential is a constant (denoted by V_0) on the drop surface, we have on the surface

$$V^s = V_0 - V^\infty$$

Now the conservation of total charge gives

$$\int \frac{\partial V^s}{\partial \mathbf{n}}\,\mathrm{d}s = -Q + E_0 \int n_z\,\mathrm{d}s$$

where s is the arclength of the generator of the axisymmetric drop. The linear system of the algebraic equations resulting from the boundary element formulation combined with the conservation of total charge allows us to solve for $V^s_{\mathbf{n}}$ and V_0.

The details of the boundary element formulation are given in Brebbia *et al.* and will not be repeated here. We comment specifically on the following.

(1) We have used linear interpolation to represent the free surface and the functions ϕ, ϕ_n, V and V_n. The disadvantage of a linear element is that the free surface is not smooth. This leads to some difficulty in evaluating the diagonal entries of the matrix $\mathbf{H}$. We avoid such complication by calculating the diagonal entries using known properties:

$$\sum_{j=1}^{N} H_{ij} = 0$$

for the hydrodynamic problem. This equation can be easily derived by using the heat conduction analogy, namely, the flux is zero if the temperature on the surface of a finite body is constant. For the electrostatic problem, which is an exterior problem, a similar equation

$$\sum_{j=1}^{N} H_{ij}^{e} = 4\pi$$

can be obtained by using the definition of the matrix **H**, where the superscript signifies the electrostatic problem.

(2) In obtaining the matrices **G** and **H**, integration of singular functions is required. While it is common practice to cut out a segment on the integration interval to evaluate singular integrals analytically, we choose to evaluate the singular integrals by using the known nature of the singularity. Without loss of generality, we can assume, due to the logarithmic nature of the singularity, that

$$A_n = \int_{\delta_n}^{a} f(x)\,\mathrm{d}x = F - \alpha\delta_n - \beta\delta_n \log \delta_n + O(\delta_n^2)$$

Then F gives an approximation accurate up to $O(\delta_n^2)$. If we choose three different values as δ_n; and numerically evaluate the integral to get A_n, the above relation yields three algebraic equations for F, α and β. For sufficiently small δ_n, the value F gives a good approximation of the singular integral.

(3) The boundary element formulation is a direct formulation in contrast with those which assume a vortex layer at the free surface such as the approach of Lundgren & Mansour (1988). The difficulty with an indirect formulation, such as the vortex sheet formulation, is that the tangential velocity of the free surface is not known for sure because it experiences a jump across the free surface. Inaccurate tangential velocities cause boundary points to accumulate at some location and remeshing is needed after a few time steps. With our direct formulation, no remeshing is needed.

(4) We have identified an important source for numerical instability. Numerical instability of the drop simulation programs has been reported by many authors. Lundgren & Mansour (1988) report that the cause of such instability is still unknown. However, we believe that the well-known instability of the Runge–Kutta method may be the cause of numerical instability in most of the existing drop calculations.

The instability of the Runge–Kutta method has been studied extensively. To understand this instability, let us consider numerical integration of the following simple ordinary differential equations:

$$\dot{x} = \omega y$$

$$\dot{y} = -\omega x.$$

These equations describe the motions of a linear oscillator and the solutions are sinusoidal functions. Indeed, sinusoidal functions are what we get from the (fourth order) Runge–Kutta method if a "small enough" time step is chosen. However, when the time step Δt exceeds $2.8/\omega$, no matter how small x and y are to start with, we always end up with exponential growth of x and y until the computer fails to continue the calculation.

The instability in the drop problem is associated with the stiff nature of our dynamical systems, see Gear (1971). The reason why it occurs in the current drop dynamics problem can be understood with some knowledge of the linear analysis of the free surface. If the deviation of the drop shape from the spherical shape is small, the dynamics of the drop can be described in terms of linear Legendre modes. If we use (x_i, y_i) to denote the two phase variables of a particular mode with mode number i, the strategy of advancing the free boundary is analogous to solving the following initial value problem

$$\dot{x}_1 = \omega_1 y_1$$

$$\dot{y}_1 = -\omega_1 x_1.$$

$$\cdots$$

$$\dot{x}_n = \omega_n y_n$$

$$\dot{y}_n = -\omega_n x_n.$$

Although we are usually interested in the behavior of a few slow modes, the fastest frequency (say ω_n) is still present. Hence the time step for stability should be controlled by the fastest mode. The fastest mode present is controled by the number of elements. Hence the more elements we use, the smaller the time step allowed by the stability requirement.

Based on this argument, we can calculate the largest time step for the drop problem with (say) 100 elements. With this number of elements, we can represent the Legendre modes up to P_{100}, which has a frequency of $1005/\sqrt{2}$, in the timescale of Lundgren & Mansour (1988). Hence the critical time step is

$$\Delta t = 2.8\sqrt{2}/1005 = 0.00394$$

With our boundary integral program, we have *numerically* identified the critical time steps for stability with n ranging from 20 to 100. The data points are shown in figure 2. The dashed line is the theoretical result based on the above argument. Note however that the natural frequency of the nth mode is estimated based on small amplitude oscillations from the spherical shape. When the shape of the drop is deformed away from the spherical shape, the natural frequency of the fastest mode can be significantly different from the above estimate. In addition, when the nodes are not evenly distributed, the time step allowed by stability considerations is often smaller than the above estimate.

We comment that the stiff system we encounter here is different from the stiff systems that are well treated by some integrators such as Gear's method. In our case, the linearized system has eigenvalues with large imaginary parts due to the oscillatory nature of the dynamics. This is in contrast with more common stiff systems which are characterized by large negative eigenvalues. By choosing sufficiently small integration time intervals ($\Delta t = 0.005$), we can avoid the instability. We therefore carry out our numerical integration using a fourth order Runge–Kutta method. We limit the number of surface elements to 40 to insure stability.

(5) We have attempted to incorporate weak viscous effects in the fluid into our program. We tried to accomplish this by including in the computation a vorticity calculation based on partial solution of the boundary-layer equations which describe the weak vortical surface layer. The solution of the vorticity equation influences the drop dynamics through the inclusion of viscous

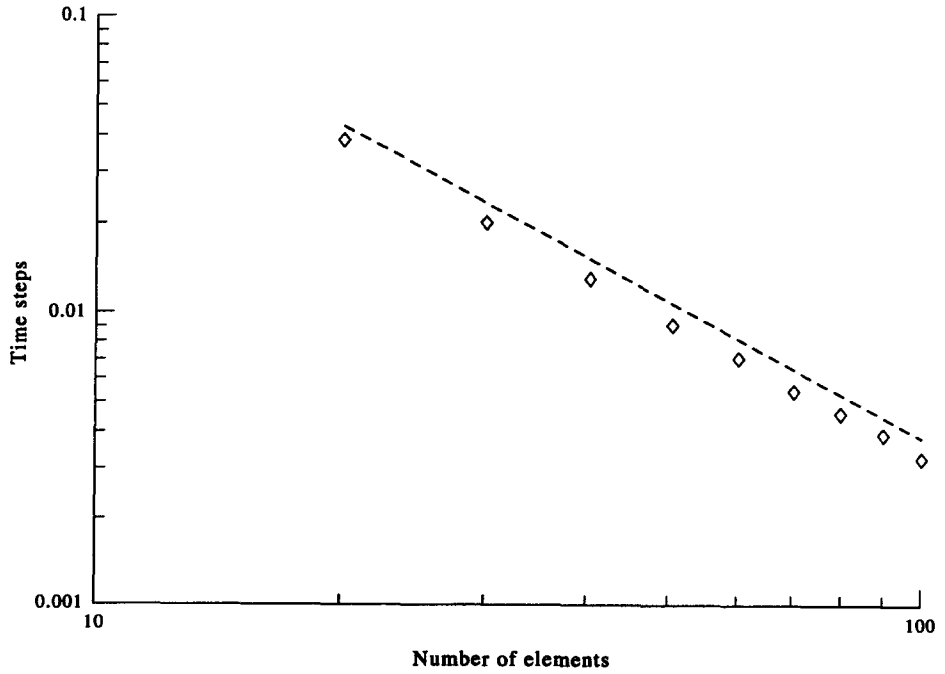

Figure 2. The dependence of the maximum integration time step upon the number of elements. The dashed line is based on $\Delta t = 2.8\sqrt{2}/\omega_n$ where n is the number of elements. The dots are the smallest time steps above which the numerical integration is interrupted by instability.

terms in the normal stress boundary condition. The details of such an approach are given in Lundgren & Mansour (1988). Unfortunately, further numerical instability is caused by such a treatment. Hence our simulation is mostly limited to inviscid drops. Since the equilibrium shape of the drop does not depend on the viscosity, we followed Lundgren & Mansour's treatment formally by incorporating just the normal stress contribution of the viscosity as in Dommermuth (1994).

4. VALIDATION OF THE NUMERICAL CODE

The computer programs we have developed for this work were checked against some numerical and analytical results. Specifically, we have done a simulation of the drop response to an initial impulse with the same initial conditions as used by Lundgren & Mansour (1988). For this purpose, our time scale has been adjusted in order to compare to their result. Our results are shown in figure 3(a)–(c). Figure 3(a) shows the time history of the position of the top end of the drop. Figure 3(b) shows the kinematic, potential and total energy defined in the same way as in Lundgren & Mansour. These results appear to be identical to the results of Lundgren & Mansour. Figure 3(c) shows the equivalent radius of the drop as a function of time. This is an indicator of whether our numerical code conserves the total volume of the drop. We find that the radius variation is less than 0.3%.

As another check of our program, we verify that the gravitational force is actually balanced by the electrostatic force, as it should be at steady state. In dimensional variables, this requires that

$$E^*\mathrm{B}^* = \frac{4}{3}\pi\rho g R^3.$$

That is

$$\mathrm{B} = \frac{3}{4\pi} EQ$$

in dimensionless variables. If we choose $E = 0.2$ and $\mathrm{B} = 0.6$; the necessary charge to maintain force balance is

$$Q = 4\pi$$

Although at that charge $Q = 12.56$, the drop is seen to drift slowly upward in our calculations, the static balance is achieved if we slightly reduce the charge to 12.54. Figure 4(a) and (b) shows the positions of the uppermost end of the drop as a function of time for the above two cases. The motion of the top end of the drop (the north pole) is composed of a contribution due to shape oscillation, and a slow drift upward in figure 4(a) [downward in figure 4(b)].

The natural frequencies of a charged drop have been calculated by Lord Rayleigh (1882). In our timescale,

$$\omega_n^2 = n(n-1)(n+2)\left[1 - \left(\frac{Q}{Q_{\mathrm{R}}^{(n)}}\right)^2\right] \qquad [12]$$

where

$$Q_{\mathrm{R}}^{(n)} = 4\pi\sqrt{(n+2)}$$

and $Q_{\mathrm{R}} \equiv Q_{\mathrm{R}}^{(2)} = 8\pi$ is the so-called Rayleigh limit. This result can be used as a further check on the accuracy of our numerical program. By carrying out numerical integrations for a certain amount of time starting with an almost spherical drop with a small P_2 perturbation of the shape, we can obtain the frequency of small amplitude oscillation by counting the number of peaks in a given time interval. In figure 5, the curve corresponds to the theoretical value for ω_2 according to [12]; the dots correspond to numerically computed values using our program.

5. THE EQUILIBRIUM SHAPE AND STABILITY OF AN ELECTROSTATICALLY LEVITATED LIQUID DROP

The equilibrium shape of an electrostatically levitated liquid drop has been studied by Adornato & Brown (1983) using asymptotic analysis and the finite element method. Even though our

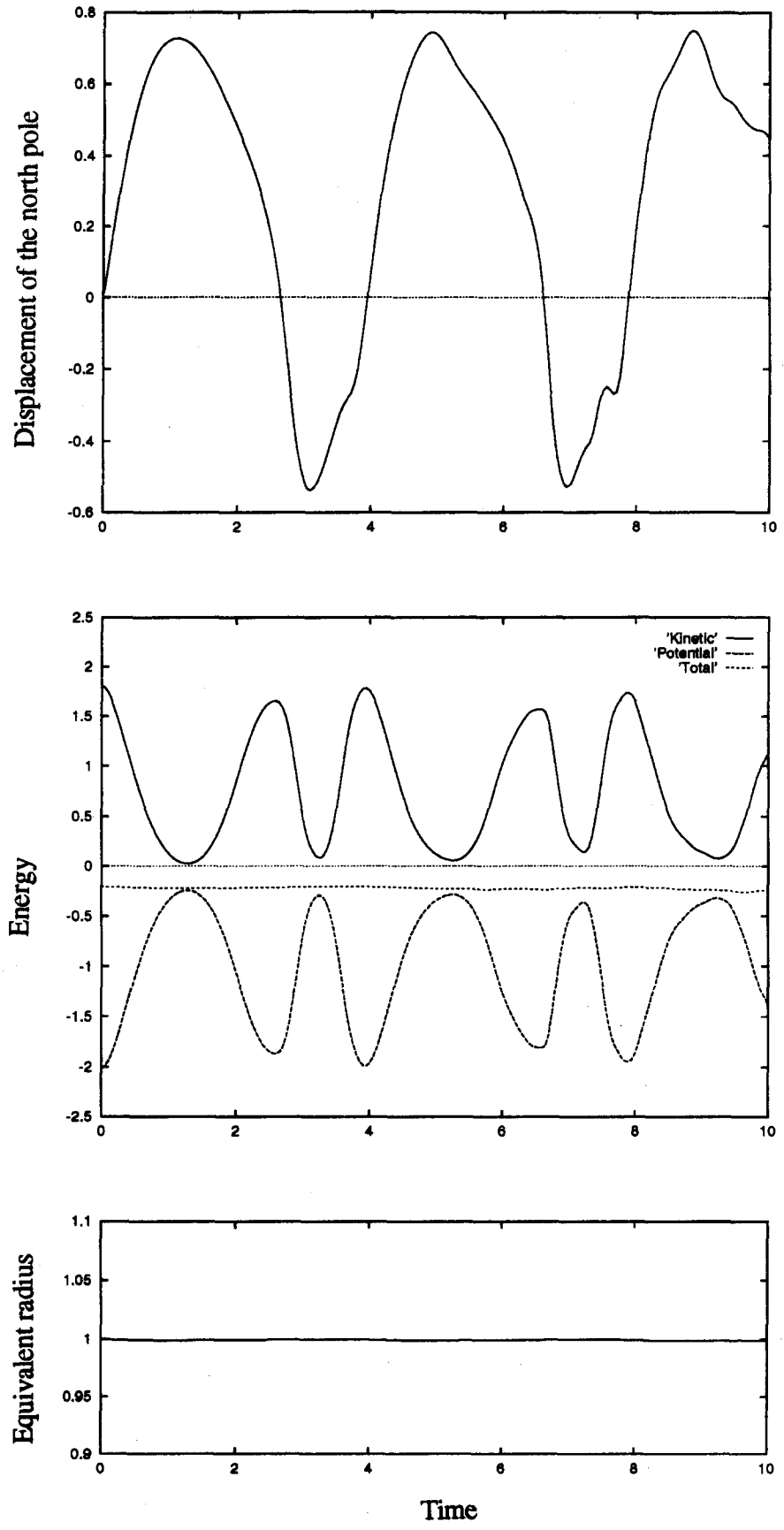

Figure 3. Second-mode oscillations with initial conditions $\phi = 0.6P_2$ and $r = 1$. The number of elements used are 40 and $\Delta t = 0.005$. (a) The displacement of the upper end of the drop (the north pole), (b) kinetic, potential and total energy and (c) the equivalent radius of the drop.

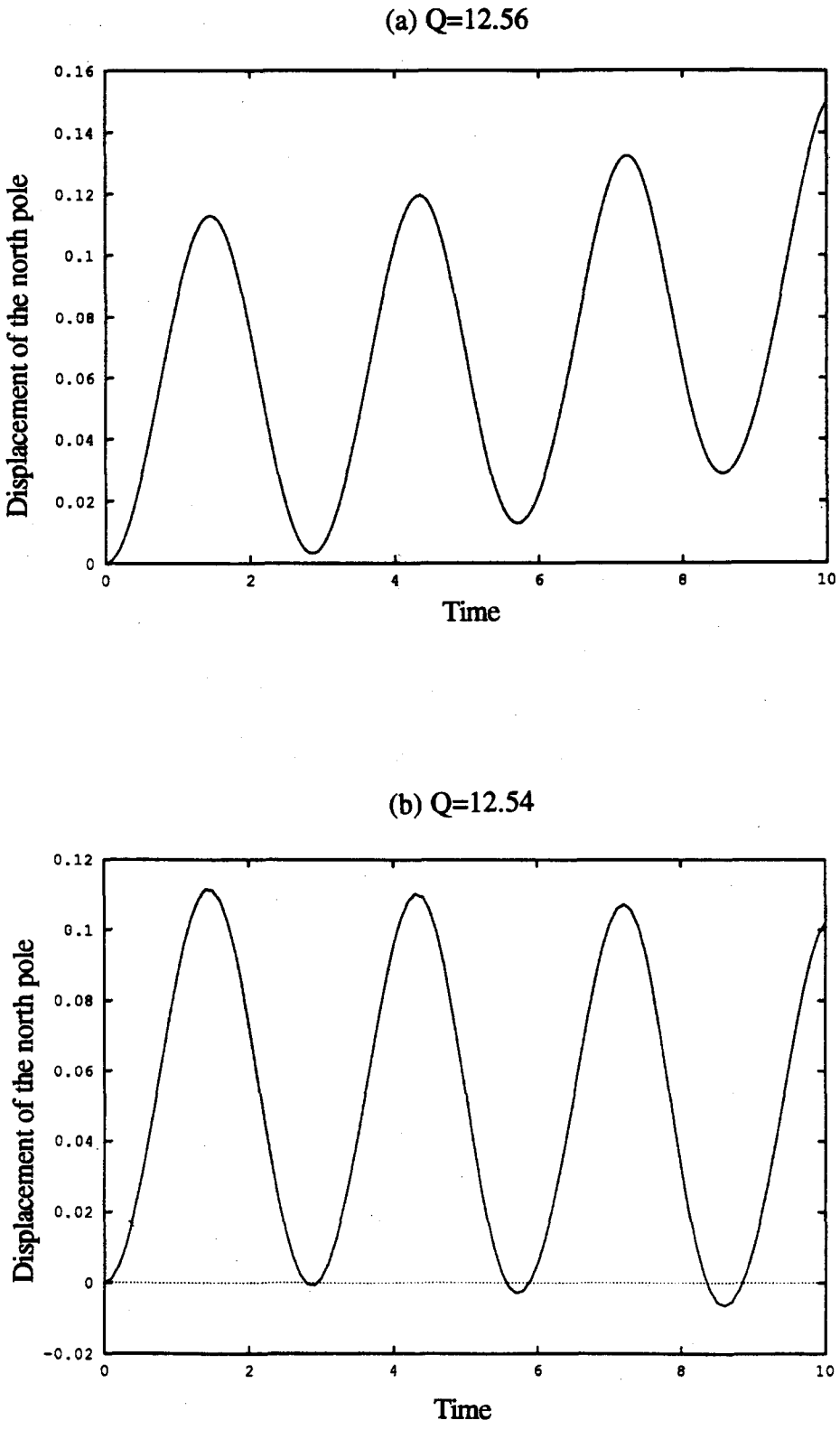

Figure 4. The displacement of the drop north pole for $E = 0.2$, B = 0.6. (a) The drop is seen to drift upwards for $Q = 12.56$ and (b) the drop drift is downwards for $Q = 12.54$.

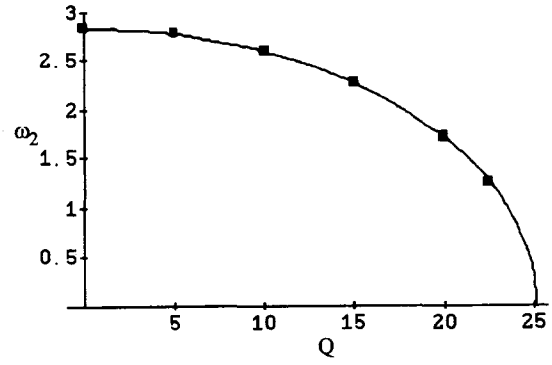

Figure 5. The natural frequency of the P_2 mode as a function of the charge on the drop. The line is based on [12] and dots are from our numerical calculation.

numerical code is best geared to study the dynamics of the drop, it is possible for us to study the equilibrium shape of the drop by including a viscous normal stress term in the dynamic boundary condition and carrying out long time integration until the drop reaches a steady state. Since the equilibrium shape of the drop is independent of viscosity, this non-rigorous treatment of viscous effects does not affect our result for the equilibrium shape.

Comparison between our result and that of Adornato & Brown is satisfactory. For example at $E = 0.3385$ (corresponding to $E = 1.2$ in the nomenclature of Adornato & Brown) the amplitude of the Legendre modes for mode numbers from zero to seven are listed in table 2. Note that the amplitudes of all modes with odd mode numbers are zero in our result. They are not zero according to Adornato & Brown. Since the mirror symmetry about the equator of the drop is preserved if the drop is subjected to an electric field alone, all odd modes should have zero amplitude. In this aspect our result is more accurate than that of Adornato & Brown.

In addition to reproducing the results of Adornato & Brown, we have done a systematic study of the dependence of the drop equilibrium shape on the levitation parameters (E, Q and B). We use the length of the long axis (i.e. the symmetry axis) to characterize the drop deformation. Since all lengths have been non-dimensionalized by the radius of an equal volume spherical drop, it is convenient to divide the drop length by two. We denote this dimensionless quantity as a. If the Bond number is not zero, the typical equilibrium shape of the drop does not exhibit mirror symmetry about the equator. It is because of this that we use the length of the drop rather than the Taylor deformation measure involving the axis ratio as an indicator of shape deformation. Figure 6 shows the half length of the symmetry axis as functions of the electric field for various values of Q. For fixed Q, the deformation increases as the electric field strength increases. The rate of increase accelerates and the curves in figure 6 approach vertical tangents as the strength of the electric field increases. Therefore, for each fixed Q, there exists a corresponding maximum value of E, above which no stable equilibrium shape of the drop exists. For $Q = 0$, this maximum is the Taylor limit, which is 0.451 based on our calculation.

As the electric charge increases, the maximum electric field for the existence of a stable equilibrium shape decreases, and the maximum achievable deformation of the drop also decreases. Since the existence of a stable equilibrium shape dictates whether a drop can be stably levitated, we plot the maximum electric field for various Q. This is represented by the data points shown in figure 7. The lower left region below these data points corresponds to regions where a drop can be stably levitated. We also show curves corresponding to constant Bond numbers,

$$\mathrm{B} = \frac{3EQ}{4\pi}$$

Table 2. Legendre modes at equilibrium

Mode number	0	1	2	3	4	5	6	7
Adornato & Brown	0.997	−0.002	0.113	0.020	0.016	0.006	0.003	0.001
This work	0.997	0.000	0.111	0.000	0.009	0.000	0.001	0.000

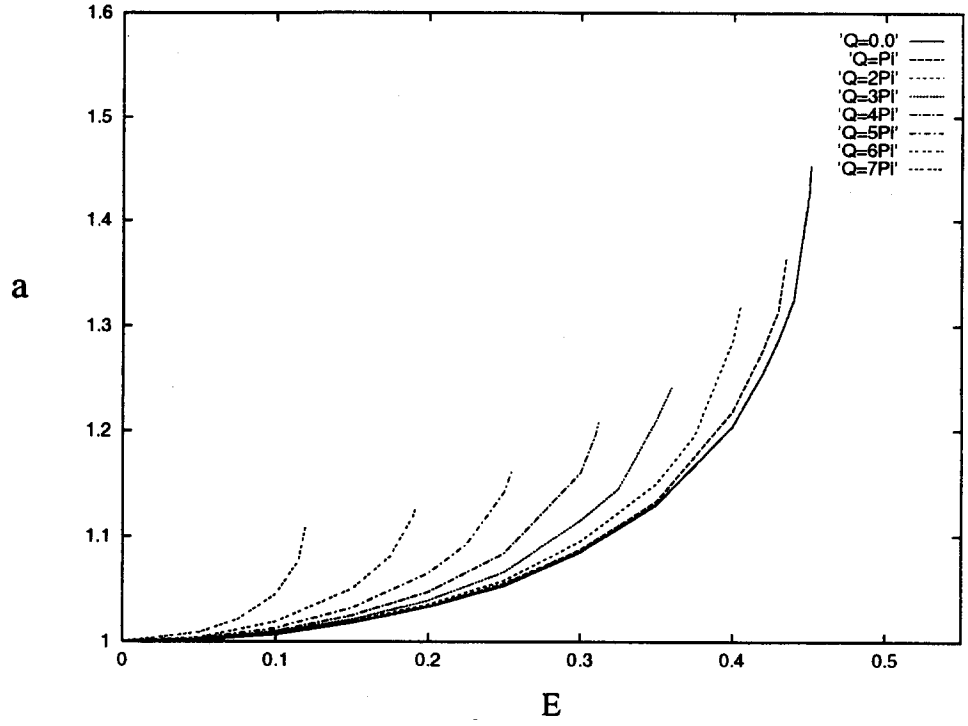

Figure 6. Dependence of the drop deformation at the equilibrium on the strength of the electric field as functions of the electric charge. The deformation of the drop is represented by the half-length of the symmetry axis.

from B = 0.2 to B = 1.0. Based on that, we conclude that the *maximum drop size* we can stably levitate has a Bond number near 0.9. This suggests that drops with Bond number approaching 0.9 become difficult to levitate. Roughly speaking, optimum parameters for levitating a drop are that E and Q are near 50% of the Taylor limit and the Rayleigh limit, respectively.

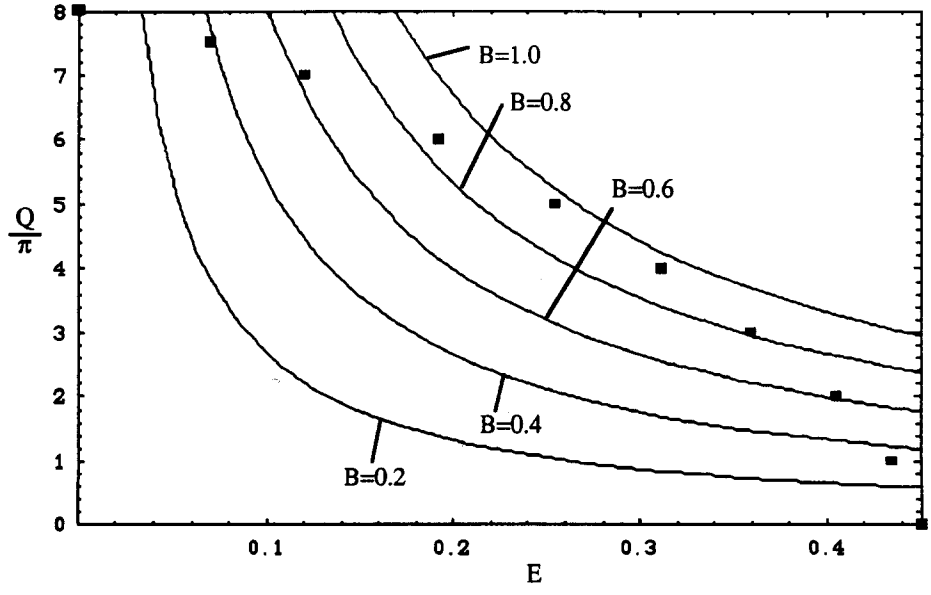

Figure 7. The region where the stable equilibrium exists. The region is defined by the square dots.

A liquid drop can be levitated using various combinations of the charge and the electric field. It is thus interesting to know how the equilibrium shape of the drop depends on the charge and the electric field. For that purpose, we have done computations at a fixed Bond number (0.6) for various values of Q and E. The results of these calculations for several representative cases are shown in figure 8. We observe that a combination of large surface charge and small electric field leads to less distortion of the equilibrium shape from that of a sphere. A combination of small surface charge and large electric field, on the other hand, leads to a large distortion of the shape; furthermore, the loss of mirror symmetry about the equator is more apparent.

It is important to realize that because of the non-linear nature of the drop dynamics problem, the drop dynamics depend strongly on initial conditions. As an illustration, for $Q = 0$, $E = 0.45$ is below the Taylor limit. Hence a stable equilibrium shape exists. However, a drop whose initial shape is a sphere will become unstable if subjected rapidly to an electric field of this strength. This is shown in figure 9 which is a plot of $\dot{a}$ versus a. We observe that the two poles of the drop develop very large velocity and the motion becomes unbounded. For this reason, it is important to recognize

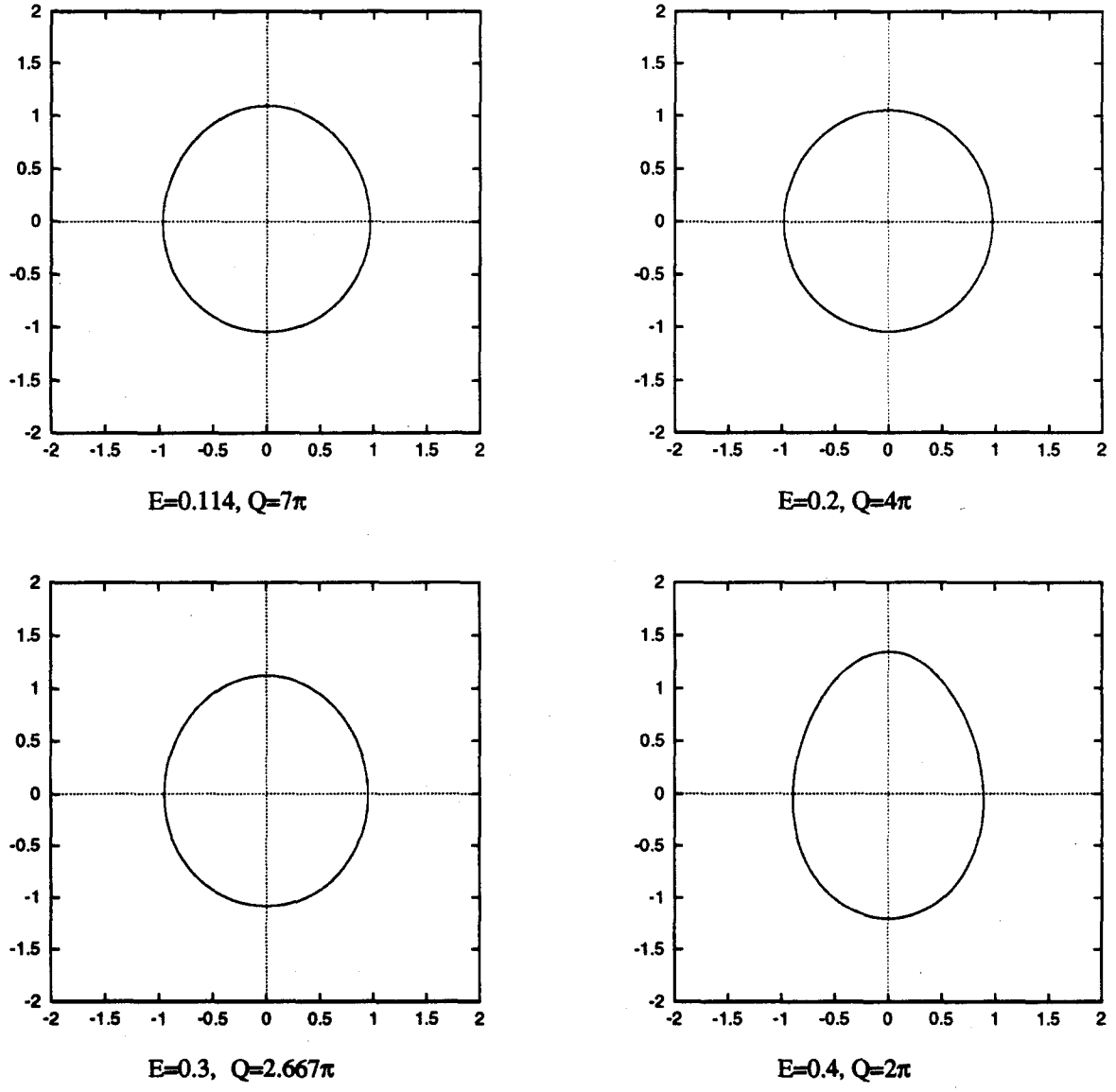

Figure 8. Stable equilibrium shapes corresponding to the same Bond number, which is 0.6, but different combinations of E and Q.

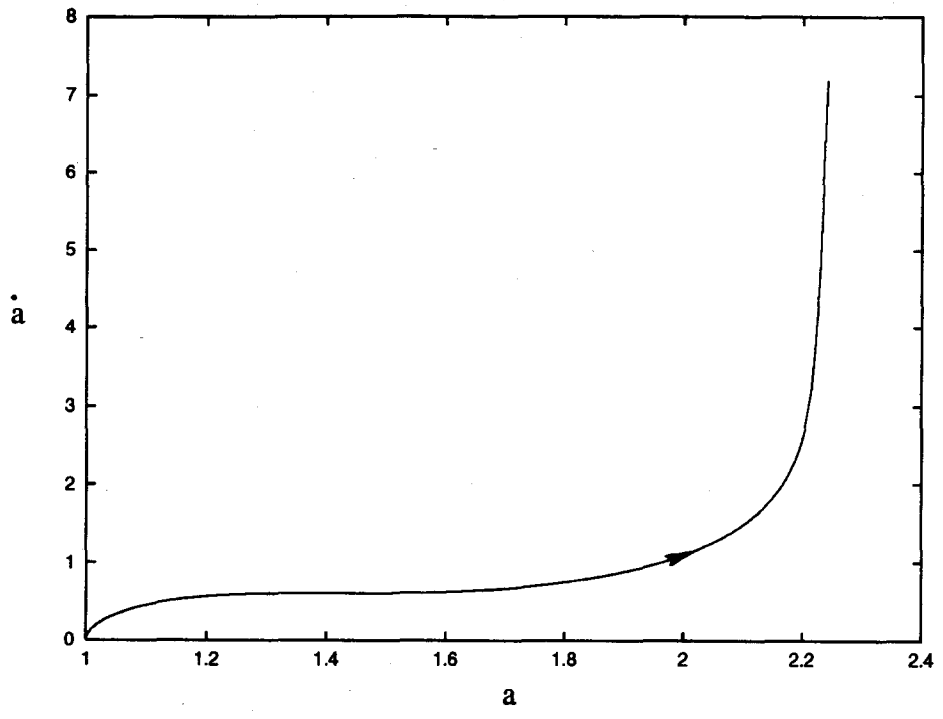

Figure 9. For $E = 0.45$, which is below the Taylor limit, the drop develops a large velocity at the two poles. The time rate of change of the half-length of the symmetry axis, $\dot{a}$, is plotted against a.

that the maximum E values in figures 6 and 7 have been obtained by incrementing through small steps in E, beginning from $E = 0$. In the above example, the stable equilibrium can be reached only if we start our calculations from a spheroid that is very close to the maximum deformation, with $a = 1.40$.

For levitation parameters and initial conditions outside the region of stable attraction to the steady state solution, the drop develops large velocities at the poles. The shape evolution of a drop as time progresses from an initial spherical shape for $E = 0.45$ and $Q = 0$ is shown in figure 10. We observe that because of large velocities at the two poles, the drop develops sharp corners at these points. Further integration of the drop dynamics is aborted because our boundary integral formulation cannot handle the impending singularity in curvature at the two poles. When both the electric charge and the electric field are present, the mirror symmetry about the equator of the drop is broken. The evolution of the drop shape from a spherical initial shape for $E = 0.4$, $Q = 2\pi$ and $B = 0.6$ is shown in figure 11. Now the drop develops a sharp corner only at one of the two poles as if the drop is suspended in the gravity field by a string attached to the north pole.

Since our code is a dynamic one, among all possible equilibrium shapes only stable equilibrium shape can be obtained. Due to the axisymmetry restriction of our program, we will also obtain equilibrium shapes that are stable under axisymmetric perturbation but unstable under non-axisymmetric perturbation. For instance, in the absence of an electric field, an oblate axisymmetric equilibrium shape has been found for charges above 8π, the Rayleigh limit. However, these axisymmetric oblate shapes have been shown to be unstable under non-axisymmetric perturbation; see Tsamopoulos *et al.* (1985).

6. OSCILLATION FREQUENCIES OF THE FUNDAMENTAL MODE OF AN ELECTROSTATICALLY LEVITATED DROP

For an electrostatically levitated drop, the presence of the electric charge and the electric field both have an effect on the oscillation frequencies. From [12], we see that the presence of the electric charge alone reduces the natural frequencies. The presence of the electric field also tends to reduce

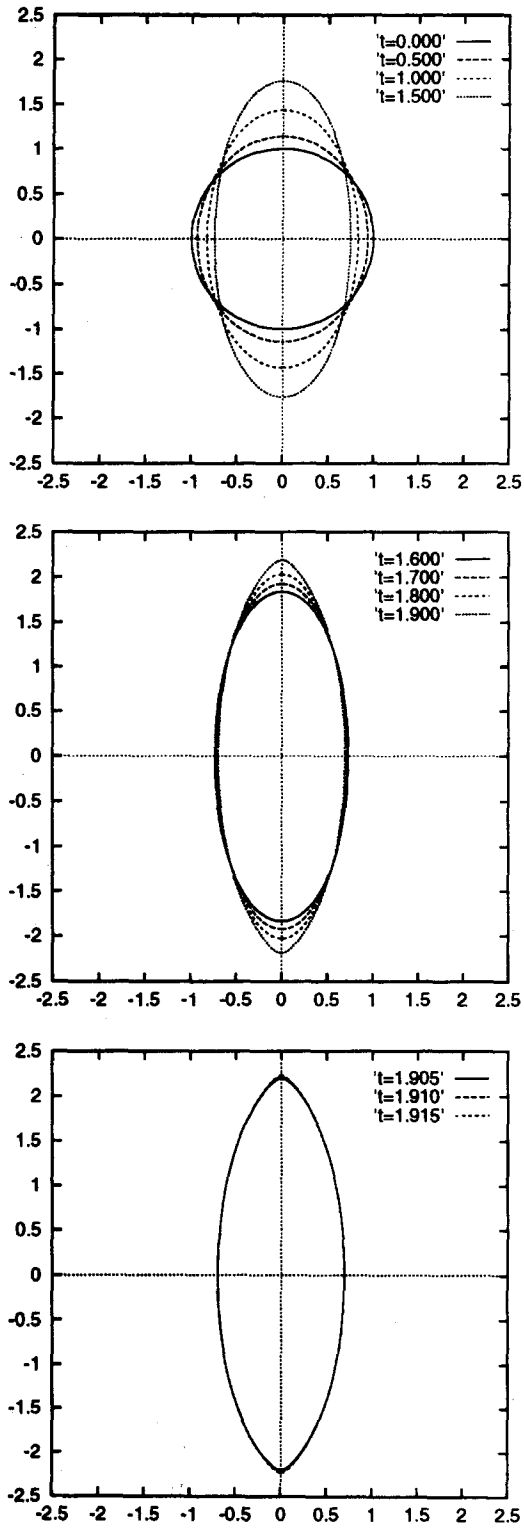

Figure 10. Development of large velocities at the two poles of the drop. Drop shapes are given at smaller and smaller time intervals for $E = 0.45$.

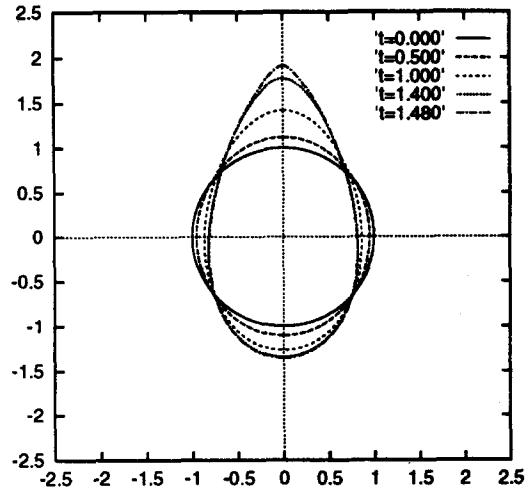

Figure 11. Drop shapes at the times given in the figure for $E = 0.4$, $Q = 2\pi$ and B = 0.6.

the natural frequencies. In addition, due to the non-linear nature of the problem, the free oscillation frequencies also depend on the *amplitude* of oscillation. In this section, we report computational results for the oscillation frequencies of the fundamental mode for various levitation parameters and oscillation amplitudes.

We compute the free oscillation frequencies of the drop by carrying out a time integration for drops with spheriodal initial shapes and fixed values of E and Q (hence B). We obtain the periods of oscillation by calculating the total time for a certain number of oscillations. To characterize the amplitude of oscillation, we could have used the amplitudes of the Legendre modes. However, since the length of the symmetry axis is more easily measured in experiments, we use $a - 1$ at $t = 0$ as the parameterization of oscillation amplitudes. We also limit our computation to $|a - 1| < 0.5$ since (strictly speaking) the motion for larger initial a is not periodic due to energy transfer to the higher modes. With this limitation on the amplitude, the motion can be reasonably regarded as periodic (amplitude variation within the first 7–10 cycles is less than 20%). For some levitation parameters, strong modal coupling occurs. As a result, the free oscillation amplitude varies substantially due to the energy transfer between modes. In these cases, accurate frequency information could not be obtained. This modal coupling will be further examined in the next section.

The results of our comprehensive calculations are shown in table 3. Missing entries in table 3 are due to the fact that for those levitation parameters and oscillation amplitudes, the amplitude

Table 3. Frequencies of free oscillation of the fundamental mode

E	Q	B	$a = 1.10$	$a = 1.20$	$a = 1.30$	$a = 1.40$	$a = 1.50$
0.0	0.0	0.000	2.825	2.797	2.732	2.673	2.605
	2π	0.000	2.721	2.684	2.631	2.579	2.521
	4π	0.000	2.431	2.399	2.350	2.292	2.235
	6π	0.000	1.860	1.829	1.782	1.747	1.691
	7π	0.000	1.347	1.310	1.261	1.202	1.147
0.1	0.0	0.000	2.789	2.754	2.703	2.631	2.569
	2π	0.150	2.684	2.648	2.602	2.550	2.486
	4π	0.300	2.383	2.344	2.291	2.230	—
	5π	0.375	2.122	2.087	2.020	—	—
	6π	0.450	1.746	1.716	—	—	—
0.2	0.0	0.000	2.647	2.615	2.562	2.513	2.449
	2π	0.300	2.555	2.528	2.483	2.432	2.368
	3π	0.450	2.415	2.395	2.347	—	—
	4π	0.600	2.168	2.140	—	—	—
0.3	0.0	0.000	2.399	2.380	2.338	2.279	2.207
	π	0.225	2.362	2.347	2.302	2.254	—
	2π	0.450	2.254	2.228	2.158	—	—
0.4	0.0	0.000	1.787	1.821	1.800	1.754	1.691
	π	0.600	1.677	1.739	1.690	1.638	—

variation of the free oscillations exceeds 20%. There are two causes for this to occur. One is due to the mode coupling between the fundamental mode and the higher modes to be further examined in the next section. The other cause is the instability of the drop equilibrium shape. Recall that for some levitation parameters the equilibrium shape can be stable with respect to small shape perturbations but unstable to large shape perturbations. This is true especially for drops levitated by large E.

Before we conduct analysis of the data in table 3, we first recall existing knowledge about the dynamics of a liquid drop, since some aspects of the dynamics of an electrostatically levitated drop are similar to those of a liquid drop in zero gravity which has been studied by various authors; see Basaran (1992) for a recent review of the papers in this area. For a liquid drop in zero gravity, the oscillation frequencies of the fundamental mode are known to depend on the oscillation amplitudes. Tsamopoulos & Brown (1983) obtain, via the asymptotic expansion method, the oscillation frequencies of the fundamental mode. As a function of the oscillation amplitude ϵ, they obtain

$$\omega = \omega_2 - 0.638\epsilon^2$$

where ω_2 is the frequency of the small amplitude oscillations given in [12] (for $Q = 0$) and ϵ is the amplitude of the fundamental mode.

Motivated by the perturbation results of Tsamopoulos & Brown, we plot the frequencies in table 3 as functions of $(a-1)^2$ for $E = 0.0$, $E = 0.1$, $E = 0.2$, $E = 0.3$ and $E = 0.4$. These plots are given in figure 12(a)–(e). The straight lines are a linear fit to the data points. Since $a - 1$ is a measure of the oscillation amplitude, we expect the frequencies to be a quadratic function of $a - 1$, at least for $a - 1$ small. For $E = 0.0$, figure 12(a), we see that the quadratic relationship is accurate up to

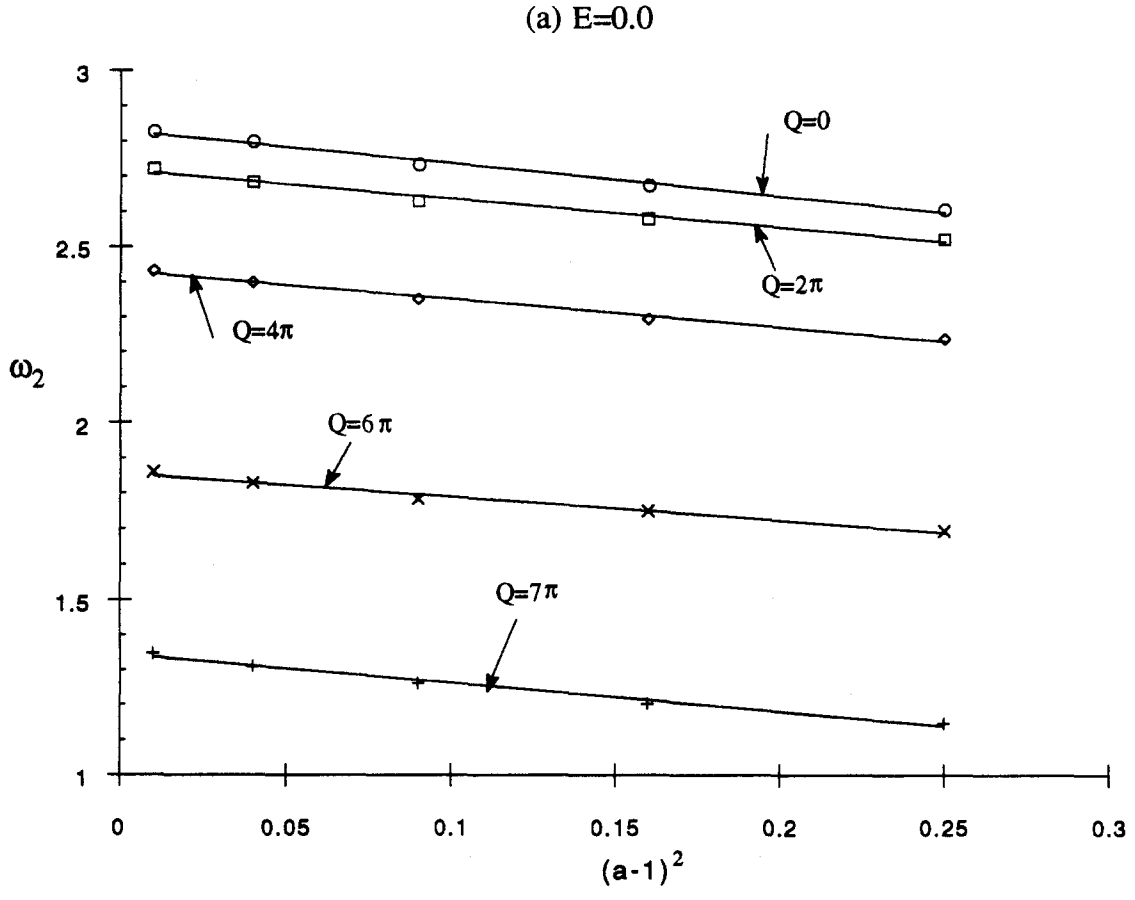

Fig. 12(a). *Caption on p. 112.*

$a = 1.5$ (the largest amplitude we have computed) and for Q between zero and 7π (recall that the Rayleigh limit is 8π). The slope based on the linear fit of the data for $Q = 0$ is 0.905. Compared with 0.638 obtained by Tsamopoulos & Brown, our result is about 30% larger. For $E \neq 0$, frequencies at large amplitudes cannot be obtained for some values of Q due to modal interactions. Otherwise, a linear relationship rather accurately captures the dependence of the frequency upon $(a-1)^2$. The slopes in all cases are negative indicating that the type of non-linearity for the drop is what is often called soft. For $E = 0.4$, a linear fit to the data points cannot be made since $a - 1$ is not a very good measure of the oscillation amplitude due to the large deviation of the equilibrium shape from the shape of a sphere.

In addition to the analytical results of Tsamopoulos & Brown, there are other results that can be used to compare with our calculations. The oscillation frequencies of the levitated drop have been calculated using asymptotic expansions by Feng & Beard (1990). Based on the formulae given in their paper, we obtain the natural frequencies of the fundamental mode of an electrostatically levitated drop in the following form:

$$\omega = \omega_2(Q)(1 - f(Q)E^2) \qquad [13]$$

where

$$f(Q) = \frac{9Q_R^2(-48Q^4 - 473Q_R^2 + 491Q_R^2Q^2)}{280(8Q^2 - 11Q_R^2)(Q^2 - Q_R^2)^2} \qquad [14]$$

When $Q = 0$, $B = 0$, the mirror symmetry of the drop about the equator is preserved, and Brazier-Smith *et al.* (1971) have obtained the oscillation frequency using spheroidal approxi-

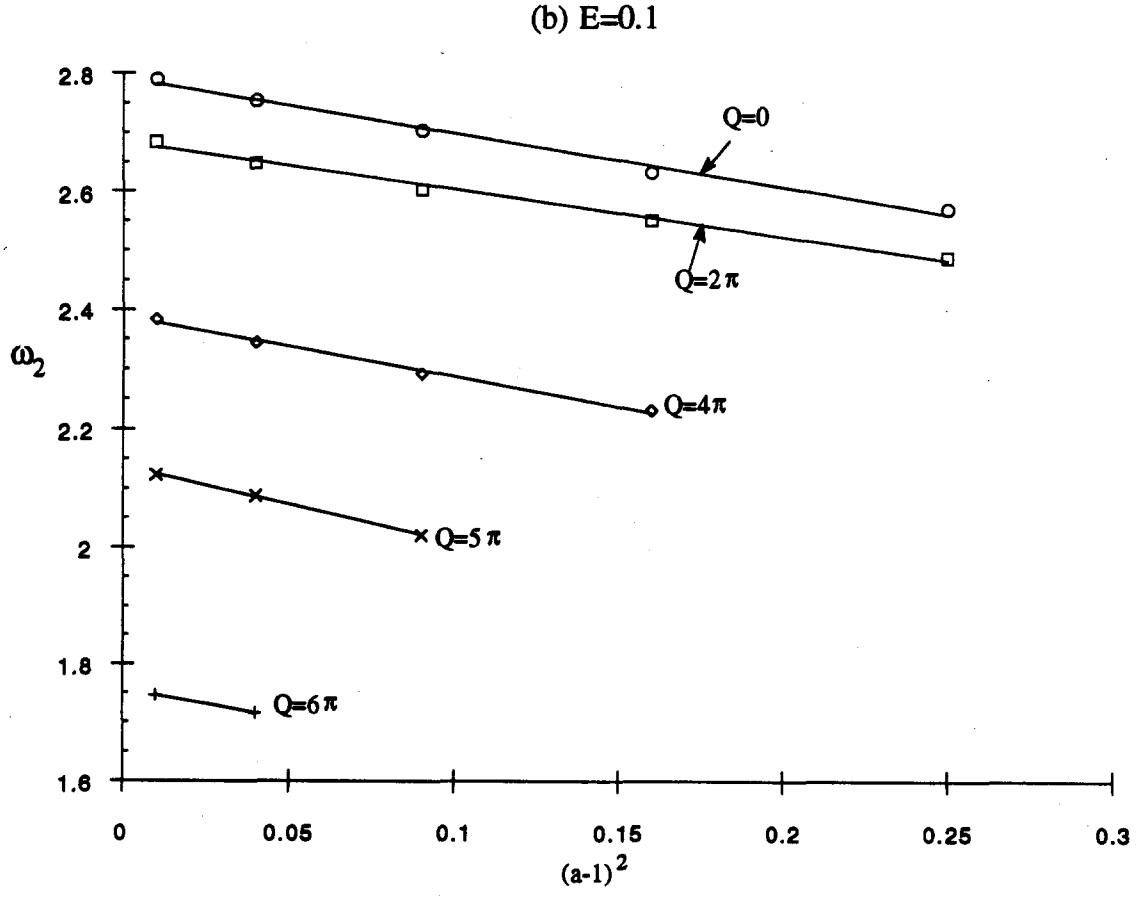

Fig. 12(b). *Caption on p. 112.*

mations. As noted earlier, the spheroidal approximation treats the drop shape as a spheroid. The length of the symmetry axis is thus a function of time. By imposing boundary conditions at the equator or at the poles, a second order ordinary differential equation is thus obtained. The oscillation frequency then follows.

Comparison of our calculations with those of Feng & Beard and Brazier-Smith *et al.* are given in figure 13(a)–(c). Figure 13(a) shows the oscillation frequency as a function of the electric field for $Q = 0$. We can see that the three results agree very well for E upto 0.3 (recall that the Taylor limit according to our non-dimensionalization is near 0.451). For E larger than 0.3, the perturbation result becomes less accurate while the spheriodal approximation result still seems to be reasonably accurate.

Unfortunately, the spheroidal approximation is not valid for $B \neq 0$ since the mirror symmetry is broken and the drop shape can no longer be captured by that of a spheroid.

As we can see in figure 13(b) and (c), for small E, the agreement between our numerical calculations and the perturbation result of Feng & Beard is very good. For relatively large E we believe that our results are currently the only accurate prediction of the resonance frequency of the fundamental mode.

7. MODAL INTERACTION

One interesting result that we discovered in our frequency calculations is that under certain levitation conditions, the Legendre modes of different mode numbers can interact with each other to give rise to amplitude modulated motions. These modal interactions provide a means by which energy can be transferred between modes and they are very important in understanding the drop dynamics.

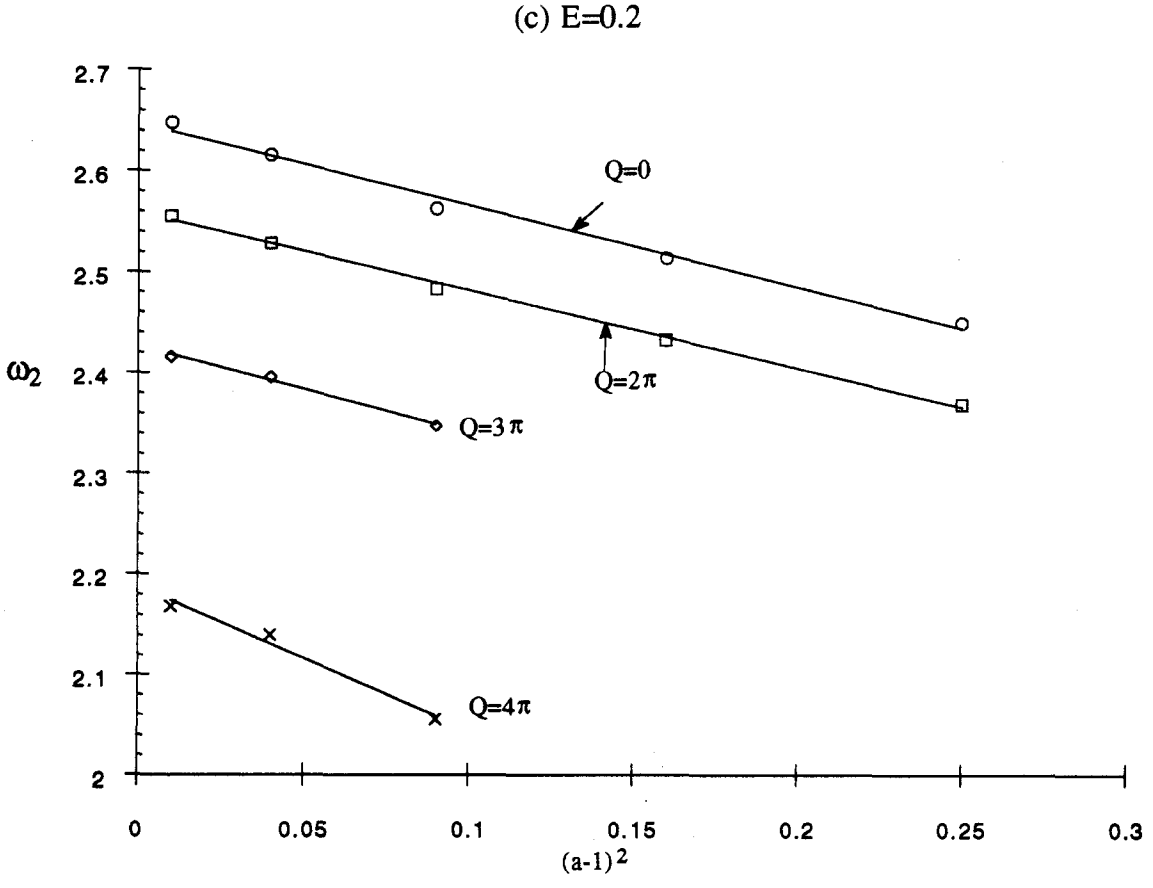

Fig. 12(c). *Caption on p. 112.*

Table 4. Natural frequencies of the first six modes at various Q

Q	ω_2	ω_3	ω_4	ω_5	ω_6
0.0	2.828	5.477	8.485	11.83	15.49
π	2.806	5.443	8.441	11.78	15.43
2π	2.739	5.339	8.307	11.62	15.25
3π	2.622	5.160	8.078	11.35	14.94
4π	2.449	4.899	7.746	10.95	14.49
5π	2.208	4.541	7.297	10.43	13.90
6π	1.871	4.062	6.708	9.747	13.13
7π	1.369	3.410	5.937	8.874	12.17
8π	0.000	2.449	4.899	7.746	10.95

A necessary condition for modal interaction at small oscillation amplitudes is that the natural frequencies of the coupled modes satisfy some resonance conditions. In the present problem, one-to-two and one-to-three resonances occur. Specifically, table 4 lists the dimensionless frequencies of modes up to mode number 6 for Q between 0.0 and 8π and $E = 0$. We see that at $Q = 0$, the frequency of the P_4 mode is three times that of the P_2 mode. We thus say that the P_2 mode and the P_4 mode satisfy one-to-three resonance conditions. At $Q = 4\pi$, the frequency of the P_3 mode is twice of that of the P_2 mode. Hence we say that the P_2 mode and the P_3 mode satisfy one-to-two resonance conditions.

The drop dynamics contains an infinite number of modes, and there is a huge number of additional resonant couplings. However, the one-to-two and the one-to-three resonances of the lower modes are more important than other types of resonant interactions since the rate at which resonant modes exchange energy is faster than any others. In addition to the two sets of resonances noted above, Tsamopoulos & Brown (1984) found that the P_4 and P_6 modes satisfy the one-to-two resonance condition for $Q = \sqrt{\frac{2}{3}}\,Q_R$.

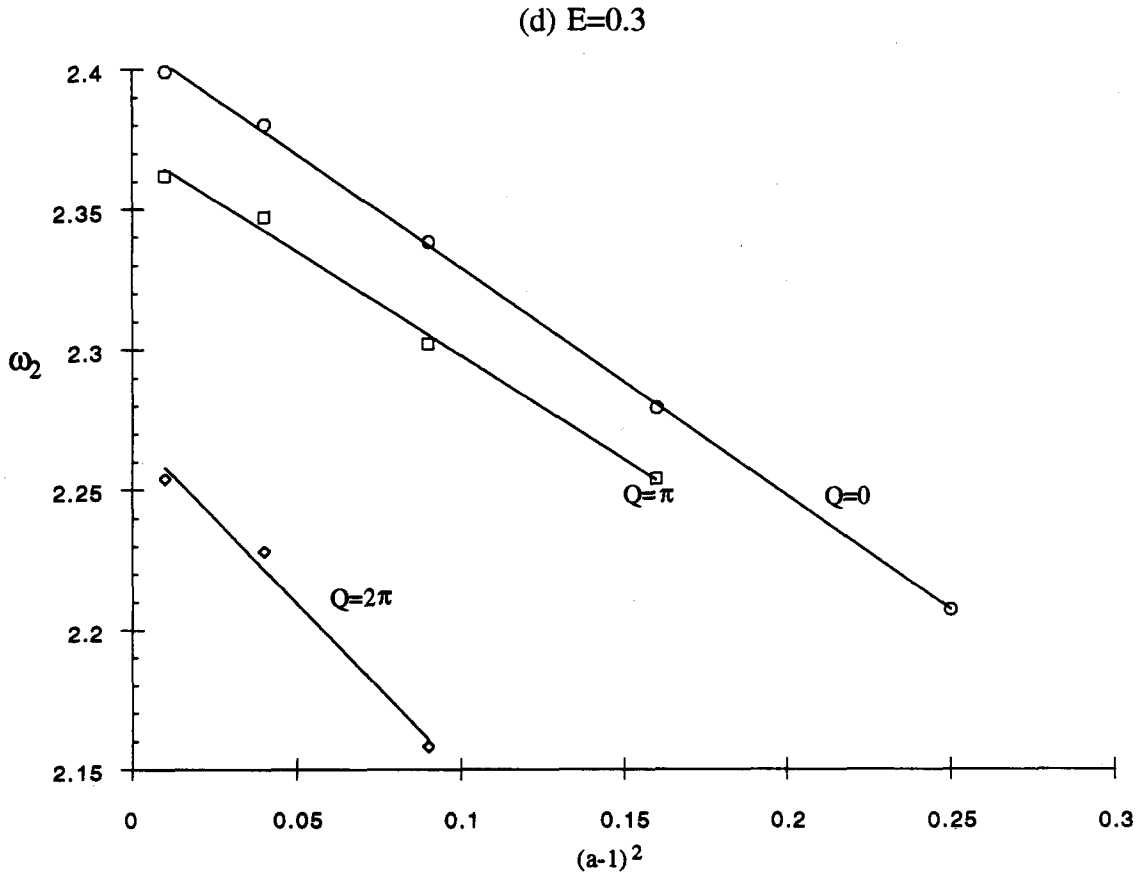

Fig. 12(d). *Caption overleaf.*

Our numerical simulation confirms the modal interactions predicted by Tsamopoulos & Brown between the P_4 and P_6 modes. We let the drop take an initial shape which has a P_4 component of amplitude 0.15. As time progresses, energy within the P_4 mode is gradually transferred to the P_6 mode. Figure 14(a) shows the amplitudes of these two modes as functions of time. When t is near 6, the magnitude of the P_6 mode reaches a maximum and that of the P_4 mode reaches a minimum. Energy then starts to be transferred back to the P_4 mode again. This process repeats with a period much longer than the period of the P_4 or P_6 oscillations.

Although exact one-to-two resonance between the P_4 and P_6 modes occurs only for $Q = \sqrt{\frac{2}{3}}\,Q_R$, the frequency ratio between these two modes is approximately one-to-two at other values of Q. Hence energy transfer between these two modes is expected to occur at these conditions also, perhaps to a less degree. Figure 14(b) shows the amplitudes of these two modes for $Q = 0$. We see that the two modes indeed interact with each other. But the extent of energy transfer is not as great as at exact resonance.

The one-to-two resonance condition is also satisfied between the P_2 and the P_3 modes when $Q = 4\pi$ as we can see from table 4. However, in the absence of the electric field, these two modes do not appear to interact with each other. This can be understood based on the perturbation approach of Tsamopoulos & Brown. One-to-two resonance is quadratic resonance, caused by quadratic non-linear terms in the boundary conditions governing the drop dynamics. Quadratic functions of the Legendre function P_2 are all orthogonal to the Legendre function P_3. Hence, these two modes cannot interact with each other. One should not conclude, based on this fact, that odd modes do not interact with even modes since it is shown by Lundgren & Mansour (1988) that the

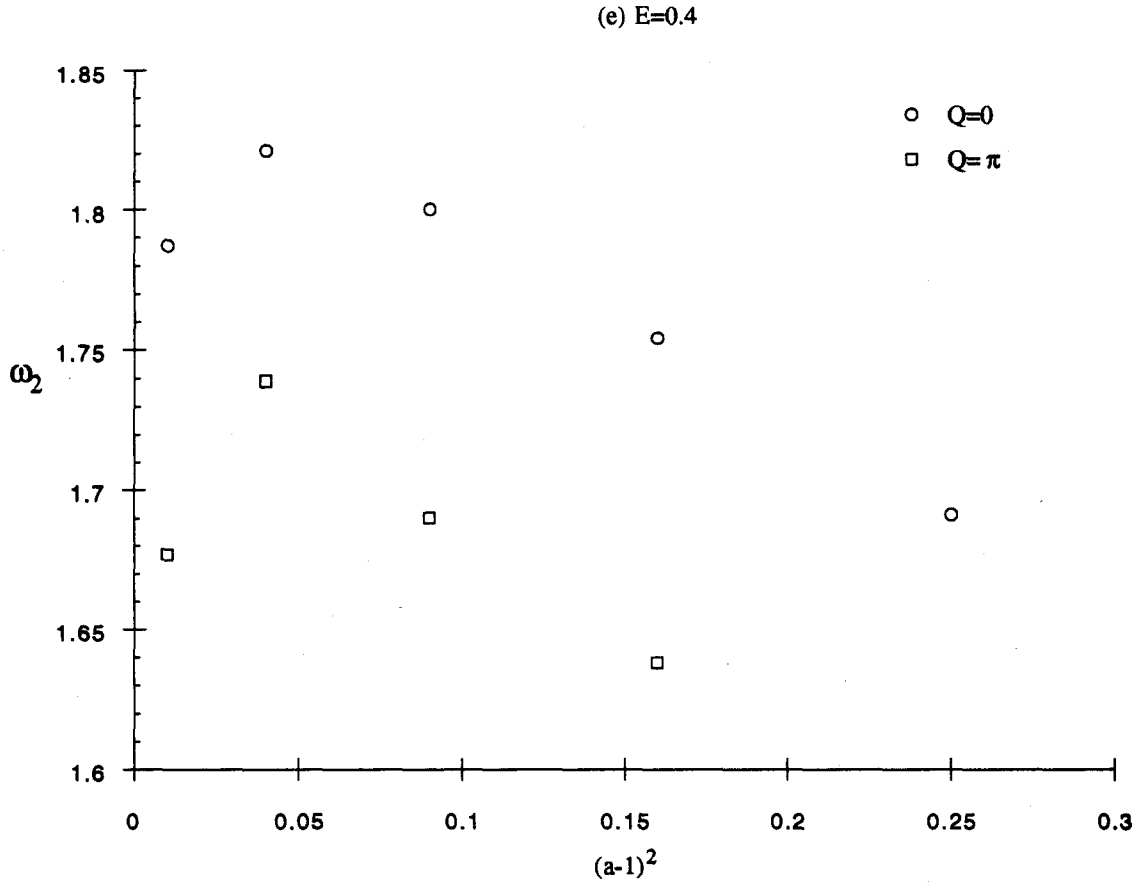

Fig. 12(e)

Figure 12. Dependence of the free oscillation frequencies of the fundamental mode on the oscillation amplitude as functions of Q. (a) $E = 0.0$, (b) $E = 0.1$, (c) $E = 0.2$, (d) $E = 0.3$ and (e) $E = 0.4$.

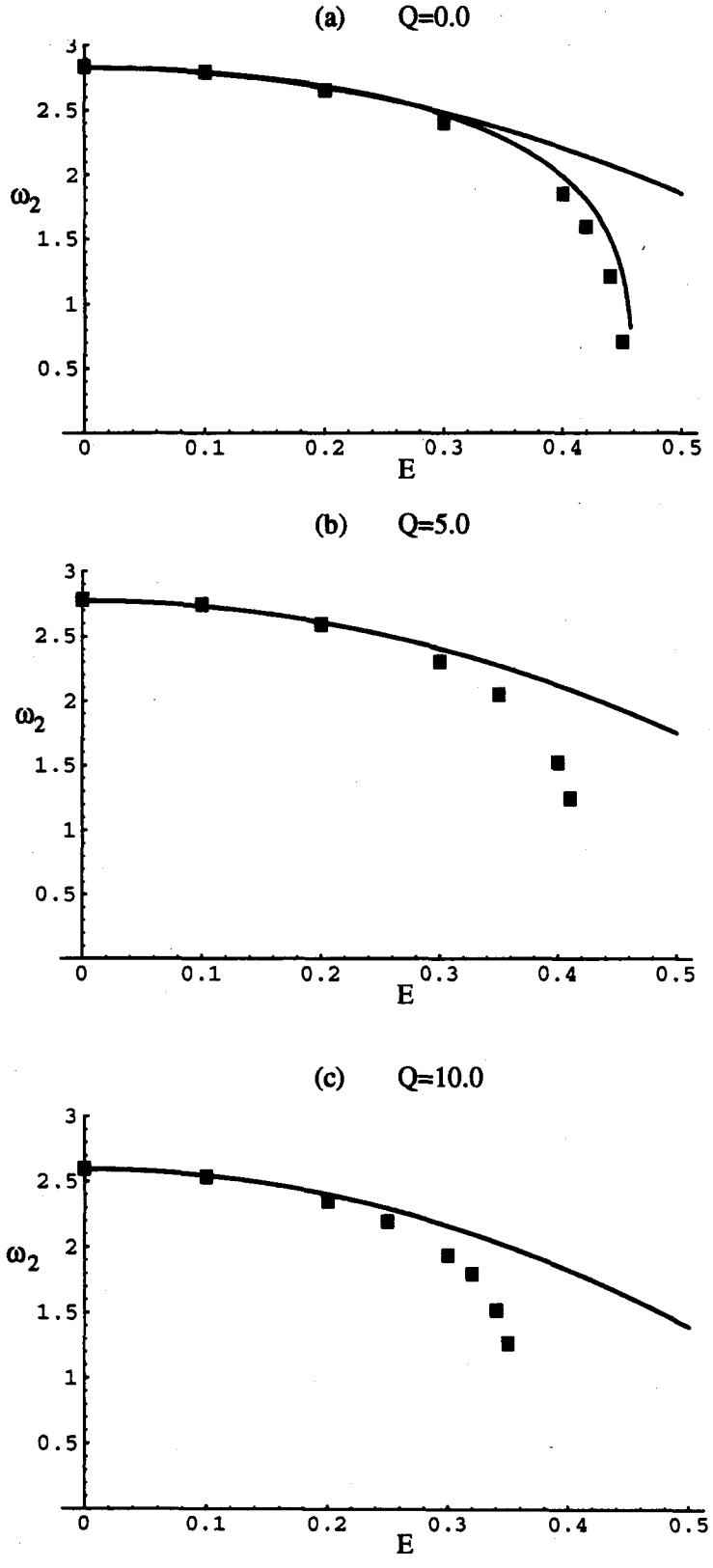

Figure 13. Dependence of the small amplitude frequencies of the fundamental mode on the electric field E. (a) $Q = 0$, (b) $Q = 5.0$ and (c) $Q = 10.0$. The square dots are from our numerical solutions and the lower line in (a) is from Brazier-Smith *et al.* (1971). Other lines are from [13] based on Feng & Beard (1990).

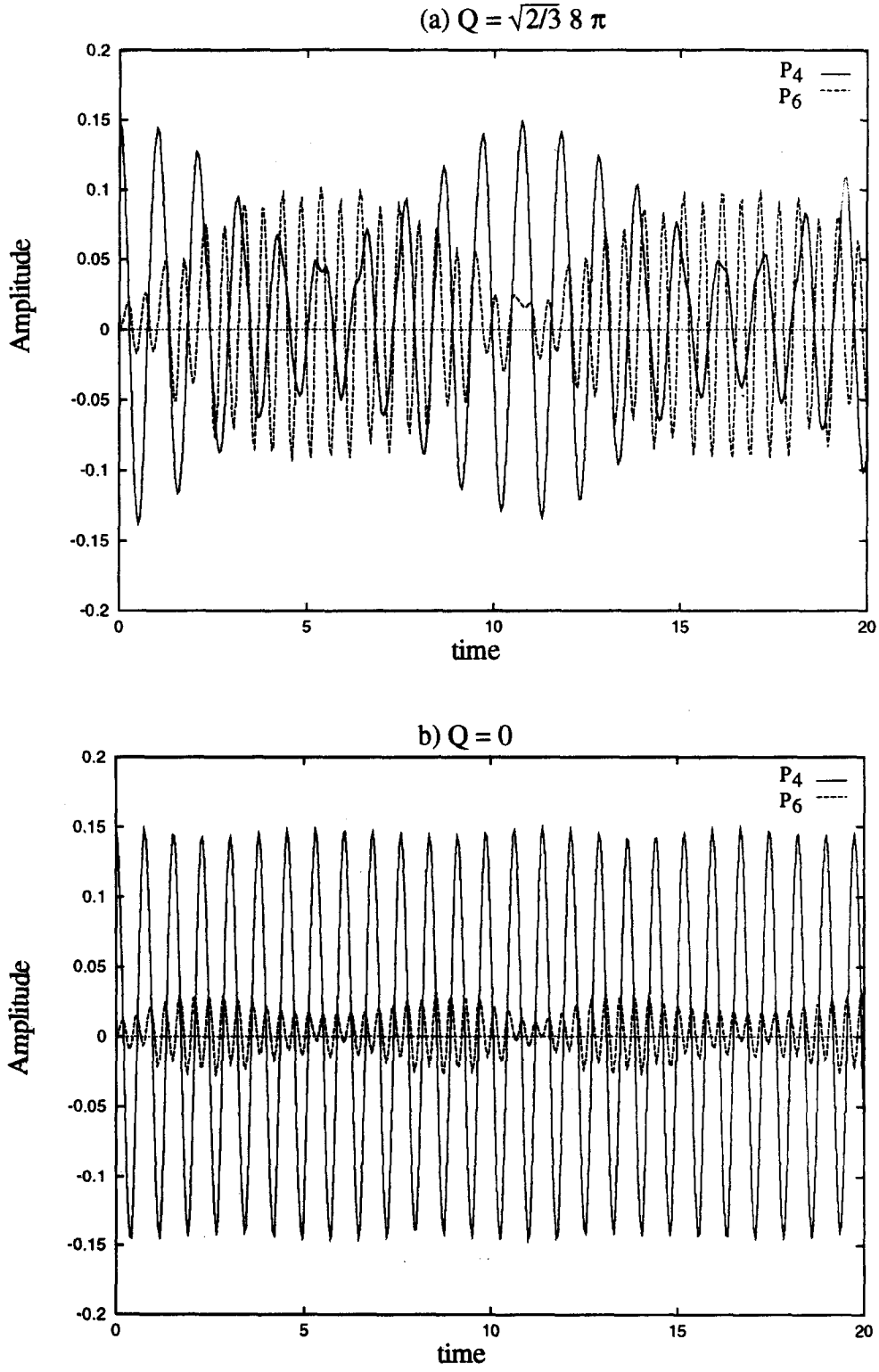

Figure 14. Modal interactions between the P_4 and P_6 modes. (a) $Q = \sqrt{2/3}8\pi$ and (b) $Q = 0$.

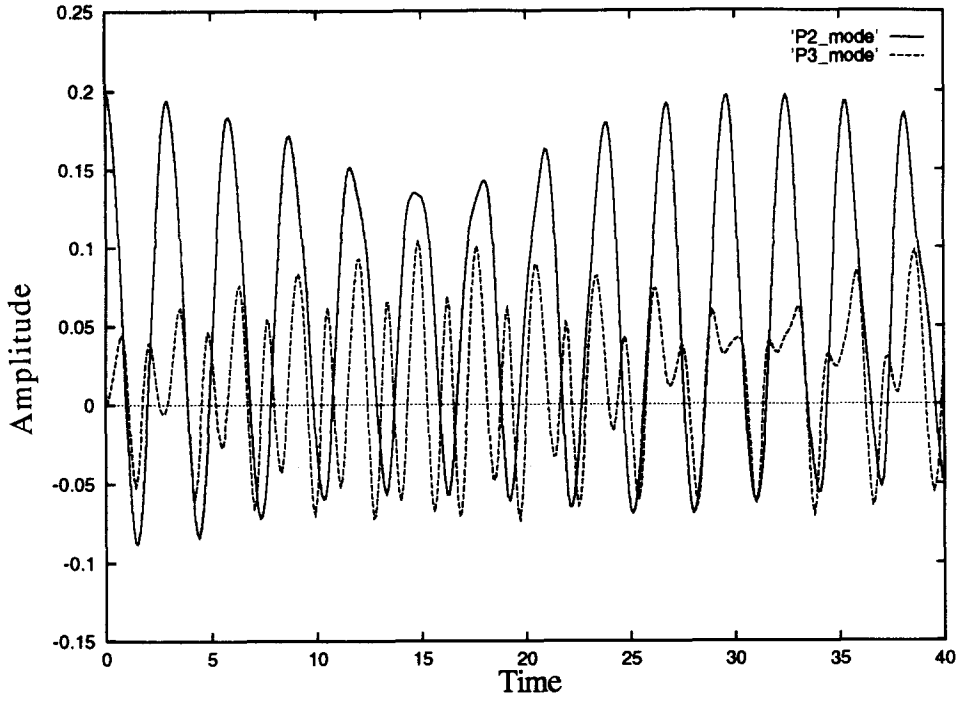

Figure 15. Modal interactions between the P_2 and P_3 modes for $Q = 4\pi$, $E = 0.2$ and $B = 0.6$. The amplitudes of both modes as functions of time are plotted.

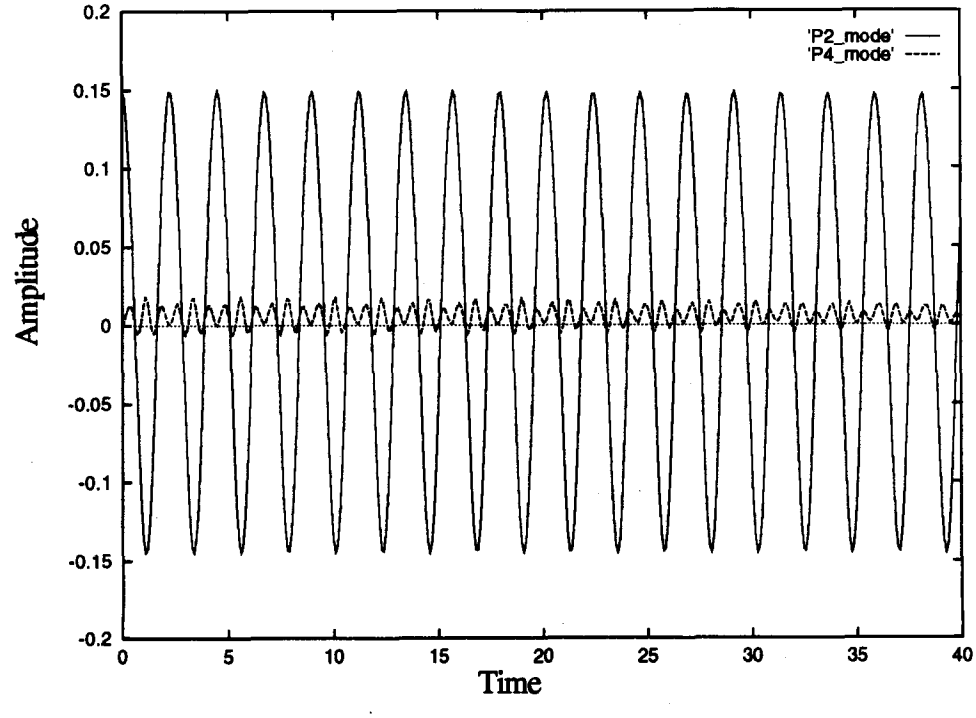

Figure 16. The modal amplitudes of the P_2 and P_4 modes as functions of time when their natural frequencies satisfy the one-to-two resonance condition.

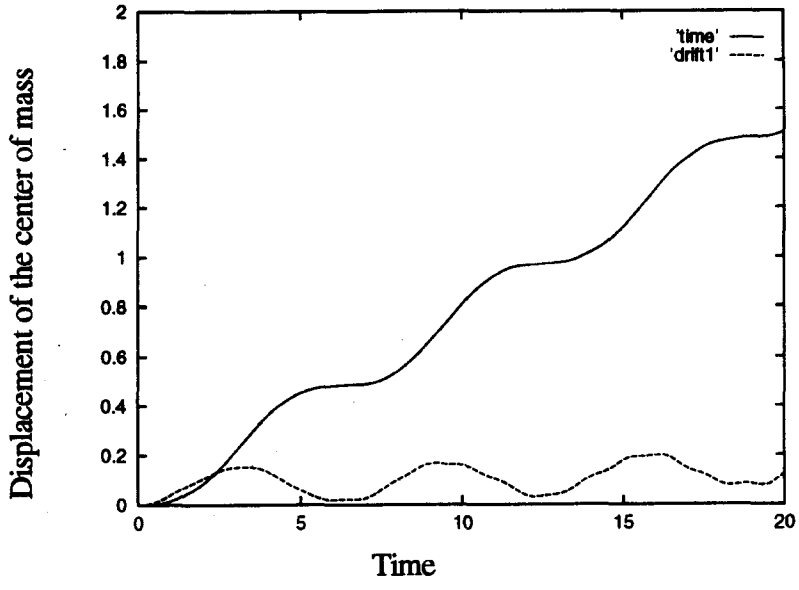

Figure 17. The upward drifts of the center of mass of the drop corresponding to different phases of the forcing. (a) $E = 0.2 + 0.05 \sin 1.0t$, $Q = 2\pi$, B = 0.3 and (b) $E = 0.2 + 0.05 \cos 1.0t$, $Q = 2\pi$ and B = 0.3.

fifth mode and the eighth mode do interact. Nevertheless, we can conclude that if the one-to-two resonant interaction is to occur between an odd mode and an even mode, the odd mode must be the slower mode.

The above argument no longer holds for an electrostatically levitated drop. For an electrostatically levitated drop, the mirror symmetry about the equator of the drop is broken. Hence the equilibrium shape of the drop contains odd order Legendre functions such as P_3, P_5 etc. The

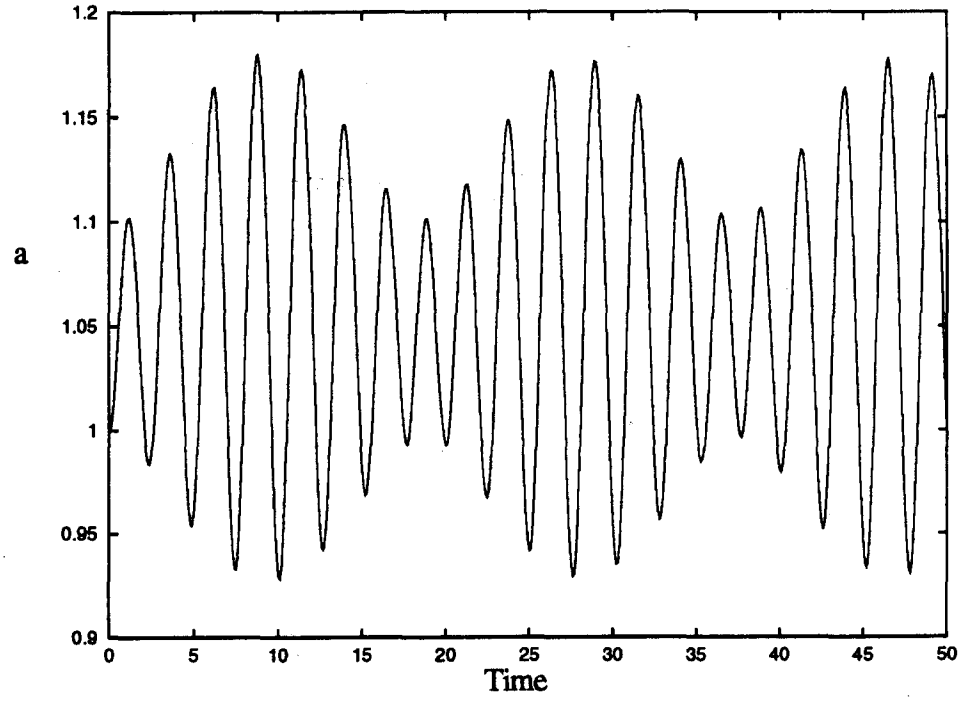

Figure 18. Oscillations of the halflength of the drop symmetry axis.

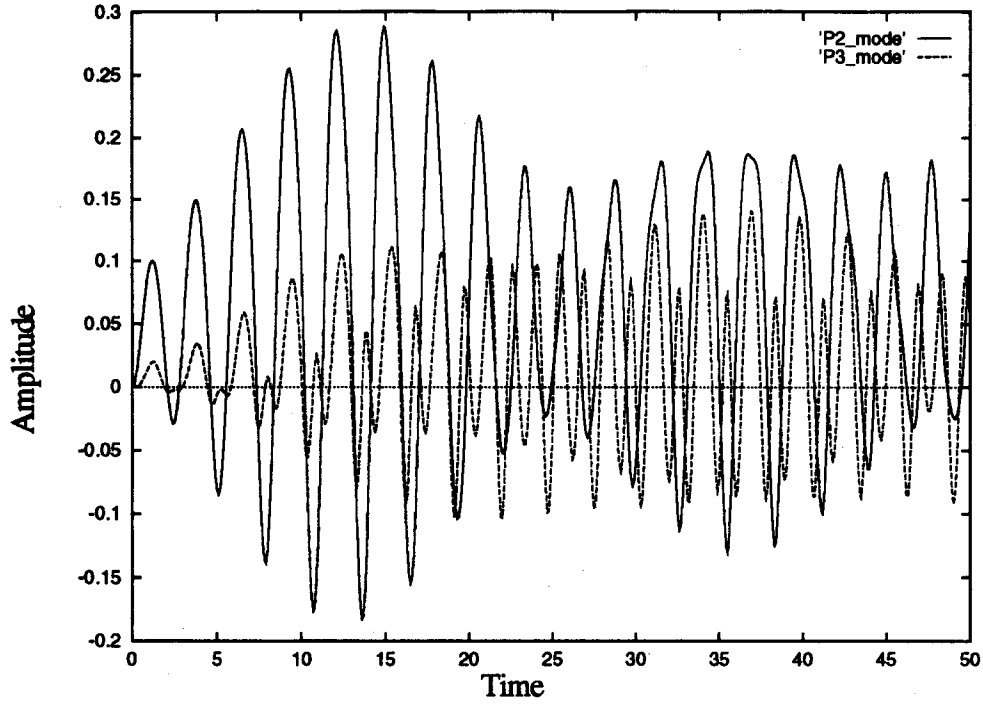

Figure 19. Amplitudes of the P_2 and P_3 modes as functions of time for $E = 0.2 + 0.05\cos 2.3t$, $Q = 4\pi$ and $B = 0.6$.

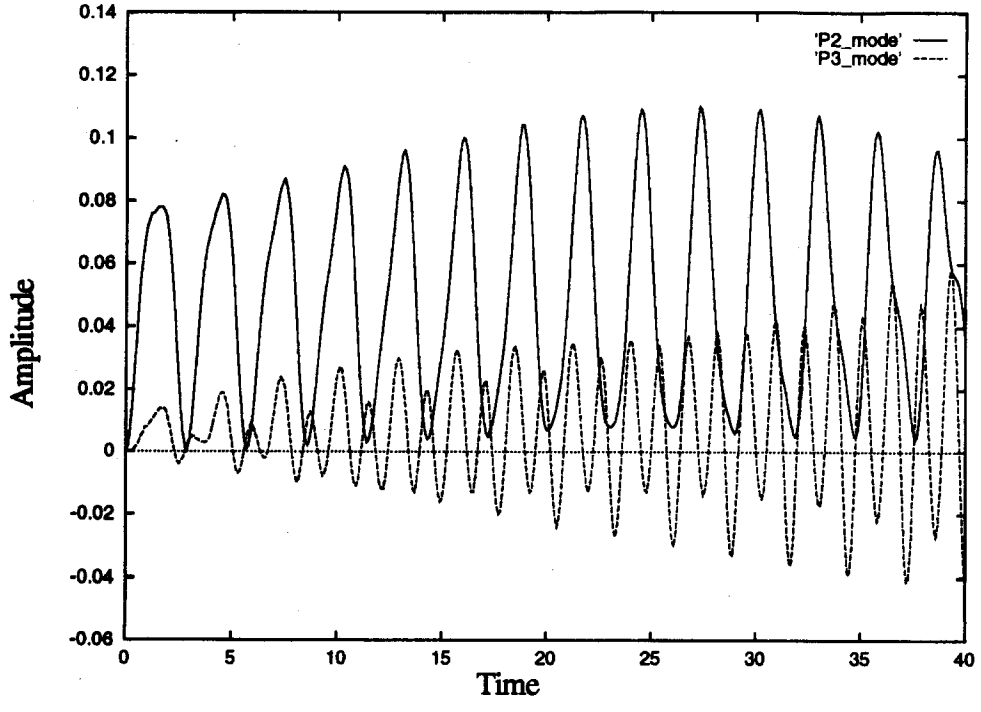

Figure 20. The excitation of the P_3 mode for $E = 0.2 + 0.05\cos 4.5t$, $Q = 4\pi$ and $B = 0.6$. The forcing frequency is close to the natural frequency of the P_3 mode.

quadratic function of P_2, P_3, P_5 etc. will no longer be orthogonal to P_3. Hence, resonant interaction between the P_2 and P_3 modes can occur.

Indeed, our numerical simulation confirms such interaction. In fact this is the most significant influence associated with non-zero Bond number on the drop dynamics. Most of the missing entries in table 3 of our frequency calculation are caused by the energy transfer between the P_2 and the P_3 modes. Figure 15 shows the amplitudes of the P_2 and P_3 modes as functions of time. The drop is released from an initial P_2 shape whose amplitude is 0.2. As time progresses, the energy from the P_2 mode is gradually transferred to the P_3 mode. Since the equilibrium shape of the drop has a component in the P_3 mode, in effect the P_3 mode is also directly forced by the P_2 mode. This is the reason why the P_3 response has a subharmonic component which has half the free oscillation frequency of the P_3 mode.

The fact that no one-to-two resonance occurs between the P_2 and P_3 modes for $\mathrm{B} = 0$ suggests that merely satisfying resonant frequency conditions does not automatically imply modal interaction. In some cases, even though the two modes are coupled, however, the coupling coefficient can be very small. An example of this is the one-to-three resonance between the P_2 and P_4 modes. We show in figure 16 the amplitudes of these two modes. No energy transfer between the two modes can be observed. Since one-to-three resonance is due to non-linear terms at cubic order, the rate at which energy exchanges between the modes is expected to be much slower. However, calculations for initial amplitude of the P_2 mode as large as 0.4 still do not show evidence of energy exchanges between these two modes. This seems to suggest that the non-linear coupling coefficient is very small. It is also possible that this coupling coefficient is zero at cubic order similar to the one-to-three resonance interactions in a vibrating stretched string as shown in Feng (1995). A theoretical calculation of this coupling coefficient would be very illuminating. However, this calculation requires second order perturbation procedures and is beyond the scope of this paper.

8. DROP DYNAMICS IN A TIME PERIODIC ELECTRIC FIELD

In a time periodic electric field, the net force on the drop is also time periodic. If we use z to denote the vertical coordinate of the center of mass of the drop, in dimensionless form, the following equation of motion governs the dynamics of the center of the mass:

$$\frac{\mathrm{d}^2 z}{\mathrm{d}t^2} = \frac{3}{4\pi} EQ - \mathrm{B} \qquad [15]$$

If $E(t) = E_0 + \delta \sin \omega t$ and $\mathrm{B} = 3E_0 Q/4\pi$, the equation becomes

$$\frac{\mathrm{d}^2 z}{\mathrm{d}t^2} = \frac{3}{4\pi} Q\delta \sin \omega t. \qquad [16]$$

The solution of this equation with stationary initial conditions is

$$z(t) = \frac{3Q\delta}{4\pi\omega} t - \frac{3Q\delta}{4\pi\omega^2} \sin \omega t. \qquad [17]$$

Note that in addition to an oscillating part, the center of mass has a non-zero upward drift velocity even though the net periodic force on the drop has a zero mean. However, if $E(t) = E_0 + \delta \cos \omega t$, the drift term disappears. These two cases are shown in figure 17 for $Q = 12.56$, $\mathrm{B} = 0.6$. Note that due to small numerical errors, the drop still experiences a slow upward drift for $E(t) = E_0 + \delta \cos \omega t$ as we have explained in section 4. But it is at a much slower rate. Since we are mainly interested in drop shape oscillations, the following calculations are done for $E(t) = 0.2 + 0.05 \cos \omega t$.

Based on [3], the electrostatic forces acting on the surface of a spherical drop are proportional to the square of $E(t)$. If we let

$$E(t) = E_0 + \delta \cos \omega t$$

then

$$E(t)^2 = E_0^2 + 2E_0\delta \cos \omega t + \delta^2 \cos^2 \omega t$$

Thus if $E_0 = 0$, the drop is subjected to a periodic forcing of frequency 2ω. If $E \neq 0$, the drop is subjected to the sum of periodic forcing of frequency ω and 2ω, respectively. Therefore, if either ω or 2ω is close to the natural frequency of the fundamental mode, we expect drop oscillations of large amplitude. On the other hand, if δ is very small and $E_0 \neq 0$, the electrostatic forcing due to the term $\delta^2 \cos^2 \omega t$ may be negligible. Our numerical investigation will be mainly focused on this latter case.

Since the time variation of the electric field is small, $\delta = 0.05$, the transient motion of the drop is very similar to that of a single degree of freedom oscillator. If the forcing frequency ω is away from the resonant frequency of the fundamental mode, the drop motion contains two frequency components. One is at the forcing frequency and the other is at the natural frequency. Hence, superposition of these two frequency components will give time modulated motion. This is shown in figure 18 for $E = 0.2 + 0.05 \cos 2.5t$, $\mathrm{B} = 0.6$, and $Q = 4\pi$, where the half length of the symmetry axis is plotted against the time. In reality, the viscous effects in the fluid would damp out the component at the natural frequency and the steady state motion would be periodic at the forcing frequency. Since viscous effects are not rigorously accounted for, we do not carry out the long time integration necessary to reach the steady state periodic motions.

When the forcing frequency is close to the natural frequency of the fundamental mode, the amplitude of the fundamental mode will grow as a linear function of time until the amplitude is so large that the non-linearity is having an effect. We have seen in the previous section that non-linearity causes coupling between the P_2 and P_3 modes. We show in figure 19 the amplitudes of these two modes for $E = 0.2 + 0.05 \cos 2.5t$, $\mathrm{B} = 0.6$, and $Q = 4\pi$. The energy transfer between these two modes leads to significant amplitude of the P_3 mode.

To decide if the time dependent electric field can excite modes other than the fundamental one, we have done simulations at frequencies close to the resonant frequencies of P_3 and P_4 modes. We find that the amplitude of the P_4 mode remains small even at the frequency where resonance is expected. At frequencies close to the resonant frequency of the P_3 mode, we do notice a significant increase of the P_3 amplitude. The amplitudes of the P_2 and P_3 modes are shown in figure 20 as functions of time.

9. DISCUSSION AND SUMMARY

The boundary element method has been used to simulate the dynamics of an electrostatically levitated drop. The dependence of the equilibrium shape of the drop upon the levitation parameters is determined. It is found that a combination of relatively large electric charge and small electric field give the least distortion of the drop shape. For large electric charge and strong electric field, no equilibrium of the drop shape exists. This limits the maximum Bond number of a levitated drop to be less than 0.9.

A comprehensive study of the dependence of the fundamental shape oscillation frequency upon the levitation parameters has produced results which at small values of the electric field agree very accurately with existing analytical results. However, the numerical results are also valid at large values of E and Q. Hence, they provide an important guide for experimental work. The frequency of the fundamental mode is also dependent on the oscillation amplitude. We find that a quadratic relationship accurately describes this dependence. For all levitation parameters, the non-linearity is analogous to an oscillator with softening non-linearity.

The presence of the electric charge and electric field influences the non-linear mode interaction. For a charged drop, an exact one-to-two resonance between the P_4 and P_6 modes is possible. More importantly, however, the P_2 and P_3 modes can undergo one-to-two mode interaction for *non-zero* Bond numbers.

Our investigation of drop dynamics in a time-dependent electric field is limited to cases where the variation of the electric field is small compared with the constant part of the electric field. For this case, we find that the drop response is very analogous to that of an oscillator. At frequencies away from the natural frequency, the drop response is very small. When the forcing frequency is near the natural frequency of the P_3 mode, the P_3 mode can become excited due to the fact that the equilibrium shape of the drop does not have the mirror symmetry about the equator. Even for this case, the response can still be regarded as small. Large amplitude oscillations of the

fundamental mode can be excited if the forcing frequency is close to the natural frequency of the fundamental mode. When this happens, energy transfer to higher modes, including the P_3 mode, takes place. Due to this energy transfer to higher modes, a rigorous treatment of viscous effects is necessary before we carry out further simulations of drop dynamics in a time dependent electric field.

REFERENCES

Adornato, P. M. & Brown, R. A. 1983 Shape and stability of electrostatically levitated drops. *Proc. R. Soc. A* **389,** 101–117.

Basaran, O. A. 1992 Nonlinear oscillations of viscous liquid drops. *J. Fluid Mech.* **241,** 169–198.

Basaran, O. A. & Scriven, L. E. 1989a Axisymmetric shapes and stability of isolated charged drops. *Phys. Fluids A* **1,** 795–798.

Basaran, O. A. & Scriven, L. E. 1989b Axisymmetric shapes and stability of charged drops in an external electric field. *Phys. Fluids A* **1,** 799–809.

Brazier-Smith, P. R., Brook, M., Latham, J., Saunders, C. P. R. & Smith, M. H. 1971 The vibration of electrified water drops. *Proc. Roy. Soc. Lond. A* **322,** 523–534.

Brebbia, C. A., Telles, J. C. F. & Wrobel, L. C. 1984 *Boundary Element Techniques: Theory and Applications in Engineering*, pp. 96–99. Springer, New York.

Dommermuth, D. G. 1994 Efficient simulation of short and long-wave interactions with applications to capillary waves. *J. Fluids Engng* **116,** 77–82.

Feng, Z. C. 1995 Does nonlinear intermodal coupling occur in a vibrating stretched string? *J. Sound Vibration* **182,** 809–812.

Feng, J. Q. & Beard, K. V. 1990 Small-amplitude oscillations of electrostatically levitated drops. *Proc. R. Soc. Lond. A* **430,** 133–150.

Feng, J. Q. & Beard, K. V. 1991a Resonances of a conducting drop in an alternating electric field. *J. Fluid Mech.* **222,** 417–435.

Feng, J. Q. & Beard, K. V. 1991b Three-dimensional oscillation characteristics of electrostatically deformed drops. *J. Fluid Mech.* **227,** 429–447.

Gear, C. W. 1971 *Numerical Initial Value Problems in Ordinary Differential Equations.* Prentice–Hall, Englewood Cliffs, NJ.

Gomez, A. & Tang, K. 1994 Charge and fission of droplets in electrostatic sprays. *Phys. Fluids* **6,** 404–414.

Guckenheimer, J. & Holmes, P. J. 1983 *Nonlinear Oscillations, Dynamical System and Bifurcations of Vector Fields.* Springer, New York.

Kang, I. S. 1993 Dynamics of a conducting drop in a time-periodic electric field. *J. Fluid Mech.* **257,** 229–264.

Lundgren, T. S. & Mansour, N. N. 1988 Oscillations of drops in zero gravity with weak viscous effects. *J. Fluid Mech.* **194,** 479–510.

Miksis, M. 1981 Shape of a drop in an electric field. *Phys. Fluids* **24,** 1967–1972.

Natarajan, R. & Brown, R. A. 1987 The role of three-dimensional shapes in the break-up of charged drops. *Proc. R. Soc. A* **410,** 209–227.

Pelekasis, N. A. & Tsamopoulos, J. A. 1990 Equilibrium shapes and stability of charged and conducting drops. *Phys. Fluids A* **2,** 1328–1340.

Rayleigh, J. W. S. Lord 1882 On the equilibrium of liquid conducting masses charged with eletricity. *Phil. Mag.* **14,** 184–186.

Rhim, W. K., Chung, S. K., Hyson, M. T., Trinh, E. & Elleman, D. D. 1987 Large charged drop levitation against gravity. *IEEE Trans. Ind. Appl.* **IA-23,** 975–979.

Taylor, G. I. 1964 Disintegration of water drops in an electric field. *Proc. R. Soc. Lond. Ser.* **A280,** 383–397.

Tsamopoulos, J. A. & Brown, R. A. 1984 Resonant oscillations of inviscid charged drops. *J. Fluid Mech.* **147,** 373–395.

Tsamopoulos, J. A., Akylas, T. R. & Brown, R. A. 1985 Dynamics of charged drop break-up. *Proc. R. Soc. Lond. A* **401,** 67–88.